2.5. Erythrocyte binding assay

Approximately 1×10^7 erythrocytes were incubated in 100 μl of PBS with 10% BSA for 1 h, washed once with PBS, and further incubated in 100 μl of PBS containing 20 μl of *P. yoelii* extract for 30 min at RT, if specific volumes were not indicated. After centrifugation, the mixture was divided into erythrocyte pellets and supernatants containing unbound *P. yoelii* RhopH complexes. Supernatants were saved for later analysis to monitor RhopH complex protein degradation. Erythrocyte pellets were washed once with PBS and incubated with 1 μg of mAb#25, #32, or #16 for 15 min on ice, washed once with PBS, and incubated with 1 μg of FITC-conjugated goat anti-(mouse IgG and IgM) antibody (Biosource Int, Camarillo, CA) for 15 min on ice in 1 ml of PBS. After washing once with PBS, erythrocyte surface fluorescence was detected by flow cytometry. All experiments were done with duplicated samples and enzyme-treated erythrocytes were used in binding assays in the same day as treatment.

To distinguish GPI-deficient and GPI-positive erythrocyte populations, erythrocyte surface GPI anchor-associated CD24 was stained with rat anti-mouse CD24 mAb (BD Biosciences, San Jose, CA) and streptavidin-phycoerythrin (PE)-Cy5 (BD Biosciences). Erythrocytes from control normal mice were stained with or without anti-CD24 mAb and used as positive controls.

2.6. Flow cytometry analysis

Erythrocytes (1×10^7) were suspended in 1 ml of PBS and surface fluorescence intensities were measured by flow cytometry using a FACSCalibur™ (Becton Dickinson, NJ) flow cytometer and analyzed using the CellQuest™ software. First, single-parameter histograms were set for FITC fluorescence of cells within the scatter gate, with a gate set on the major erythrocyte population, and conditions were adjusted using untreated erythrocytes. Then, the geometric means of the fluorescence intensities were obtained for 10,000 erythrocytes incubated with or without *P. yoelii* extracts. Binding of the RhopH complex to the erythrocyte surface were given as a value obtained by dividing the geometric mean of fluorescence intensity of the experimental samples (with extract; INT_{exp}) by that of the control samples (without extract; INT_{ctl}).

For dual staining with FITC and PE-Cy5, erythrocytes were divided into two populations by PE-Cy5-fluorescence intensity and geometric mean of FITC fluorescence intensity increase were measured in these two populations independently.

2.7. SDS-PAGE, Western blot analysis, and immunoprecipitation

Parasite extracts were separated by electrophoresis on a 5–20% gradient polyacrylamide gel (ATTO, Japan) under non-reducing conditions and transferred to 0.22 μm PVDF membranes (Bio-Rad, Hercules, CA). Proteins were detected by immunostaining with corresponding antibodies, followed by horseradish peroxidase-conjugated goat antibody (anti-mouse IgG and IgM; Biosource Int) and visualized with ECL-plus (Amersham Biosciences) on RX-U film (Fuji, Japan).

To immunoprecipitate *Py*RhopH complexes, 50 μl of *P. yoelii* extract, 2 μl of yeast-produced recombinant Pys25 (yPys25) solution (5 mg ml^{-1}), and 2 μl (1 mg ml^{-1}) of mAb#32 were mixed and incubated at RT for 2 h with gentle rocking. Twenty microlitres of 50% Gamma Bind Plus Sepharose (Amersham Biosciences) solution were added and incubated another 1 h at RT with gentle rocking. The mixture was centrifuged at 21,600 × *g* for 5 min and supernatants were removed. The beads were washed in NETT [50 mM Tris (tris(hydroxymethyl)aminomethane)–HCl, 0.15 M NaCl, 1 mM EDTA, 0.5% Triton X-100, pH 7.5] + 1% BSA, NETT, high salt NETT (0.5 M NaCl), NETT, and 1/3 NETT (0.05 M NaCl and 0.17% Triton X-100). Supernatants were removed and bound proteins were eluted from beads by boiling at 100 °C for 3 min in 1× SDS-PAGE loading buffer and electrophoresed on a 5–20% gradient polyacrylamide gel under reducing and non-reducing conditions. As a control, mAb#16 was used to precipitate yPys25, instead of mAb#32.

2.8. Indirect immunofluorescence assay

A mouse harboring 28% GPI-deficient erythrocytes was inoculated intraperitoneally with *P. yoelii* 17X (lethal) and thin blood smears were prepared 3 days later at two time points. Blood smears were kept at −80 °C until use. Smears were fixed with 1% formaldehyde/PBS at RT for 15 min, blocked with 5% skim milk/PBS for 15 min at RT, reacted with rat anti-mouse CD24 mAb for 15 min at RT, washed with ice-cold PBS for 5 min, and reacted with FITC-conjugated goat anti-(rat IgG + IgM) mAb (BD Biosciences) for 15 min. Parasite nuclei were stained with DAPI (4′,6-diamidino-2-phenylindole; Wako) and mounted with Prolong Antifade solution (Molecular Probes, Eugene, OR). High-resolution image capture and processing were done using a fluorescence microscope (BX50; Olympus, Japan) and digital camera (IM500; Leica, Germany). Images were processed using Adobe Photoshop (Adobe Systems Inc., San Jose, CA).

2.9. Statistical analysis

The Mann–Whitney test was used to evaluate differences observed in erythrocyte binding assays. The chi-square test was used to evaluate the differences of parasite infectivity between GPI-positive and GPI-deficient erythrocytes. The Wilcoxon-Rank Sum test was used to evaluate the differences in parasite maturation.

3. Results

3.1. Flow cytometry analysis of PyRhopH complex interactions with erythrocytes

Prior to performing flow cytometry binding assays the character of parasite extracts was validated by Western blot analysis. *Py*RhopH2, *Py*RhopH3 and yPys25 [recombinant *Py*s25 protein (yPys25) was added to the parasite extracts as an internal control] could be detected by Western blot analysis using mAb#25, #32 and #16, respectively (Fig. 1A). *Py*RhopH1A and *Py*RhopH2 were co-precipitated using mAb#32, indicating that at least a partial RhopH complex is likely stable in the extract solution. *Py*RhopH1A, *Py*RhopH2 and *Py*RhopH3 were not co-precipitated with mAb#16 (Fig. 1B). Using parasite extracts the ability of *Py*RhopH complexes to bind normal, treated, and null erythrocytes was assessed by flow cytometry. Increased fluorescence intensity was detected using mAb#25 and #32 following incubation of BALB/c mouse strain erythrocytes with *P. yoelii* extract, in comparison to that without extract. No surface fluorescence increase was detected with mAb#16 recognizing control protein yPys25 (Fig. 1C). Fluorescence intensity increased in proportion to the amount of added *P. yoelii* extract, as shown in Fig. 1D.

3.2. PyRhopH complex binds specifically to mouse, but not rabbit or human erythrocytes

To determine the specificity of *Py*RhopH complex binding to erythrocytes, we examined binding using a panel of erythrocytes from other mouse strains [DBA/2 and B6], rabbit and human. The results were summarized in Table 1. Binding to DBA/2 and B6 mouse strain erythrocytes was similar to that from BALB/c mice. No binding was observed with rabbit or human erythrocytes with up to 50 μl of extract ($P < .01$). Thus *Py*RhopH complex recognized erythrocyte surface receptors from at least three different mouse strains, but not rabbit or human erythrocytes.

3.3. The erythrocyte PyRhopH complex receptor is sensitive to trypsin and chymotrypsin treatment

To characterize erythrocyte surface proteins involved in *Py*RhopH complex recognition, BALB/c and DBA/2 mouse erythrocytes were treated with trypsin or chymotrypsin. Both

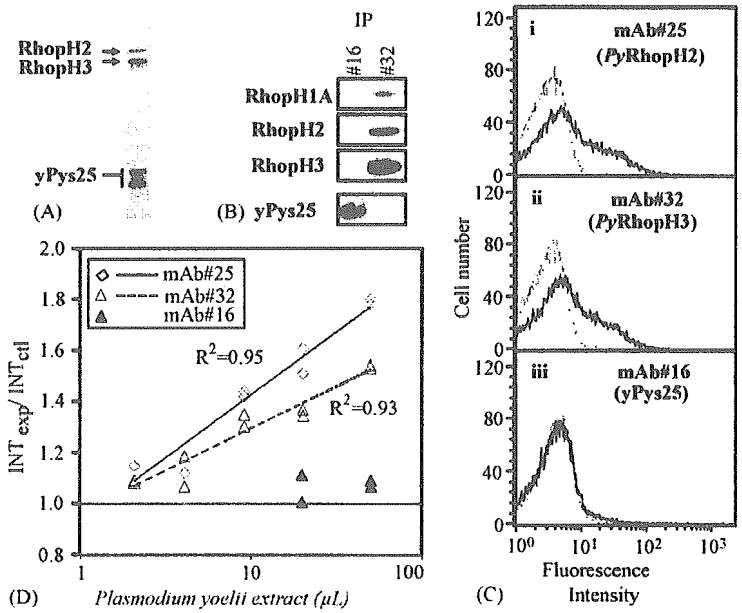

Fig. 1. *Py*RhopH complex binds mouse erythrocytes. (A) *P. yoelii* extracts were mixed with recombinant yPys25 (*Py*extract + yPys25) and subjected to Western blot analysis under non-reducing condition. The proteins were immunostained with mouse monoclonal antibodies mAb#25, #32 and #16, recognizing *Py*RhopH2, *Py*RhopH3 and yPys25, respectively. (B) Immunoprecipitation (IP) from *Py*extract + yPys25 with mAb#16 and #32 and immunostained with anti-*Py*RhopH1A mouse serum, mAb#25, #32 or #16, recognizing *Py*RhopH1A, *Py*RhopH2, *Py*RhopH3 or yPys25, respectively. The rhoptry protein complex was detected only with precipitants of mAb#32 but not mAb#16. (C) Mouse erythrocytes were incubated with *Py*extract + yPys25 (solid line) or PBS (broken line). RhopH complex binding was detected using mAb#25 or #32, followed by FITC-conjugated goat anti-(mouse IgG + IgM) antibody. A single-parameter histogram was set for FITC fluorescence of cells within the scatter gate, with a gate set on the major erythrocyte population. Fluorescence intensity increases (erythrocyte binding of *Py*RhopH complex) were observed for mouse erythrocytes with mAb#25 (i) and #32 (ii), but not with control mAb#16 that recognize yPys25 (iii). (D) The fluorescence intensity detected with mAb#25 and #32 for mouse erythrocytes increased in proportion to the amount of added *P. yoelii* extract. Representative data of multiple experiments are shown. Erythrocytes were incubated with 2, 4, 9, 20 and 50 μl of *P. yoelii* extracts and fluorescence intensity increases were measured. Geometric means were obtained for fluorescence intensities of 10,000 erythrocytes incubated with or without *P. yoelii* extract. RhopH complex binding to the erythrocyte surface was given as a value obtained by dividing the geometric mean of fluorescence intensity of the experimental sample (with extract; INT_{exp}) by that of the control sample (without extract; INT_{ctl}). Trendlines were drawn for these experiments, for which the coefficient of determination (R^2) were 0.95 (mAb#25) and 0.93 (mAb#32). Fluorescence intensities did not increase when mAb#16 was used.

Table 1
The *Py*RhopH complex binds erythrocytes of several mouse strains, but not human or rabbit erythrocytes

Erythrocyte		n[a]	INT_{exp}/INT_{ctl}[b]: median (range)	
Mouse	BALB/c	10	1.47 (1.10 – 1.80)	
	DBA/2	6	1.57 (1.38 – 1.84)	
	C57BL/6	8	1.39 (1.03 – 2.58)	
Rabbit	#1	10	0.995 (0.87 – 1.21)	
	#2	4	0.99 (0.97 – 1.04)	
Human	#1	8	1.01 (0.95 – 1.07)	
	#2	6	0.985 (0.94 – 1.04)	

[a] n indicates number of experiments and values were obtained from duplicated samples for each experiment. Data using mAb#25 were shown. Similar results were obtained using mAb#32 (not shown).
[b] *Py*RhopH complex binding to the erythrocyte surface were given as a value obtained by dividing the geometric mean of fluorescence intensity of the experimental samples (with extract; INT_{exp}) by that of the control samples (without extract; INT_{ctl}).
[c] Significant differences are indicated ($P < .01$).

Table 2
*Py*RhopH complex binding to mouse erythrocytes is abolished by trypsin- or chymotrypsin-treatment

Erythrocyte	INT_{exp}/INT_{ctl}[a]					
	mAb#25			mAb#32		
	BALB/c	BALB/c	DBA/2	BALB/c	BALB/c	DBA/2
Trypsin	0.97, 0.99	0.98, 1.04	0.99, 1.06[b]	0.91, 1.00	1.00, 1.00	0.97, 1.01[b]
Soy bean trypsin inhibitor	1.78, 1.91	1.24, 1.25	1.45, 1.47	1.75, 1.77	1.16, 1.19	1.25, 1.35
Chymotrypsin	0.97, 1.01	0.97, 0.97	1.00, 1.01[b]	1.04, 1.05	0.97, 0.98	0.98, 0.99[b]
TPCK	1.47, 1.52	1.09, 1.21	1.42, 1.57	1.40, 1.55	1.15, 1.27	1.33, 1.39

[a] *Py*RhopH complex binding to the erythrocyte surface were given as a value obtained by dividing the geometric mean of fluorescence intensity of the experimental samples (with extract; INT_{exp}) by that of the control samples (without extract; INT_{ctl}).
[b] Statistical differences ($P < .01$) are indicated between two groups using combined data from three experiments.

enzymes abolished *Py*RhopH complex binding ($P < .01$), indicating that a trypsin and chymotrypsin-sensitive erythrocyte receptor is likely involved in *Py*RhopH complex recognition (Table 2).

Involvement of the NANA component of erythrocyte surface proteins in *Py*RhopH complex recognition was evaluated using neuraminidase-treated erythrocytes. The efficiency of sialic acid removal was confirmed by the reduction of WGA lectin binding; specifically, to 17–24% or 20–24% of untreated erythrocytes following treatment of 100 or 200 mU ml^{-1} neuraminidase, respectively. Three independent experiments showed that *Py*RhopH binding was similar between controls and neuraminidase-treated erythrocytes, indicating that NANA was not involved in receptor recognition (not shown).

3.4. *PyRhopH complex binds to erythrocytes null for GPA and DARC*

Because the erythrocyte receptor is likely a membrane-associated protein, we were interested in determining if the known malaria parasite receptors GPA or DARC have roles as *Py*RhopH complex erythrocyte receptors. For these studies we used knockout mice disrupting these gene loci, in which the lack of the GPA or DARC expression have been confirmed [18,19]. Results of 4–5 independent experiments indicated that *Py*RhopH binding to GPA or DARC null erythrocytes was similar to binding of wild type erythrocytes, suggesting that neither GPA nor DARC are *Py*RhopH complex receptors (not shown).

3.5. *PyRhopH complex does not bind to the GPI-deficient mouse erythrocytes*

To evaluate the involvement of GPI anchors in *Py*RhopH complex binding, we used two mice harboring about 28% or 5% of GPI-deficient erythrocytes, which was determined with the surface expression of CD24. Erythrocytes from each mouse were separated into two groups based upon CD24-positivity, and *Py*RhopH complex bindings were independently measured. FL1 fluorescence intensity was increased for the GPI-positive population (Fig. 2A, upper), whereas it

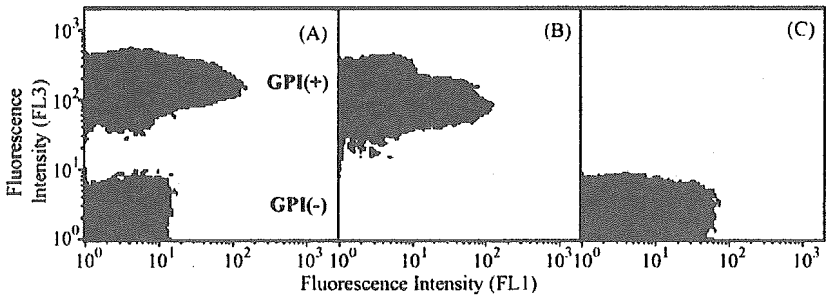

Fig. 2. *Py*RhopH complex binding to GPI-deficient erythrocytes. Representative density plot results of *Py*RhopH complex binding to GPI-deficient erythrocytes from a mouse harboring 28% GPI-deficient erythrocytes. Cell populations incubated with or without *P. yoelii* extracts are distinguished by red or blue coloring, respectively. No shift in FL1 fluorescence intensity was observed for the GPI-deficient erythrocyte population (A, lower), whereas the GPI-positive erythrocyte population shifted (A, upper). Erythrocytes from control mice stained with or without PE-Cy5 are shown as positive controls for *Py*RhopH complex binding for the upper (B) or lower (C) region. The density plot images were overlaid using Adobe Photoshop.

Table 3
The *Py*RhopH complex does not bind to GPI-deficient erythrocytes

Erythrocyte	Area	Status	INT_{exp}/INT_{ctl}[a]			
			Exp. #1[b]	Exp. #2	Exp. #3	Exp. #4
Chimeric Mouse	Upper	GPI (+)[c]	1.14, 1.14	1.33, 1.34	1.20, 1.36	1.18, 1.19[d]
	Lower	GPI (−)	0.96, 1.06	1.03, 1.04	0.97, 1.02	0.99, 1.01
Control Mouse	Upper	GPI (+)	1.21, 1.41	1.13, 1.26	1.21, 1.32	1.14, 1.19
	Lower	GPI (−)	1.18, 1.25	1.35, 1.36	1.19, 1.19	1.20, 1.21

[a] *Py*RhopH complex binding to the erythrocyte surface were given as a value obtained by dividing the geometric mean of fluorescence intensity of the experimental samples (with extract; INT_{exp}) by that of the control samples (without extract; INT_{ctl}).
[b] Experiments 1 and 2 were performed using a mouse with 28% GPI-deficient erythrocytes and experiments 3 and 4 using a mouse having 5% GPI-deficient erythrocytes. Data using mAb#25 were shown. Similar results were also obtained using mAb#32 (not shown).
[c] GPI (+) indicates GPI-positive and GPI (−) indicates GPI-deficient erythrocytes.
[d] Statistical differences ($P < .01$) are indicated between two groups using combined data from four experiments.

was not increased for the GPI-deficient population (Fig. 2A, lower). *Py*RhopH complex binding to control wild type erythrocytes were detected either with or without anti-CD24 mAb as shown in Fig. 2B and C. FL1 fluorescence intensity was not increased for negative control human erythrocytes (not shown). Experiments were done twice for each mouse and the results were summarized in Table 3. These data indicated that *Py*RhopH complex binding to GPI-deficient erythrocytes was reduced to an undetectable level using our flow cytometric binding assay.

3.6. GPI-deficient erythrocyte is resistant for P. yoelii invasion, but supports normal growth

To evaluate parasite invasion and growth in GPI-deficient erythrocytes, a mouse harboring 28% GPI-deficient erythrocytes was infected with *P. yoelii* 17X (lethal). When parasitemias reached 3.5% (smear #1) and 4.8% (smear #2), assayed by Giemsa stains of peripheral blood smears, the infection rates were independently evaluated for GPI-positive and GPI-deficient erythrocyte populations. Parasites iden-

Table 4
Invasion and development of *P. yoelii* parasites in GPI-deficient erythrocytes

Smear[a]	Status	Counted erythrocytes	Infected erythrocytes	Stage[b]		
				Early T	Late T	Schiz
#1	GPI (+)[c]	4534	159 (3.51%)[d,e]	107 (2.36%)	50 (1.10%)	2 (0.04%)
	GPI (−)	5962	100 (1.38%)	80 (1.34%)	17 (0.29%)	3 (0.04%)
#2	GPI (+)	3077	153 (4.97%)[e]	104 (3.38%)	45 (1.45%)	4 (0.13%)
	GPI (−)	3666	100 (2.73%)	66 (1.80%)	32 (0.87%)	2 (0.05%)

[a] Blood smears were made from an infected mouse when parasitemias reached 3.5% (smear #1) and 4.8% (smear #2).
[b] Representative images for each stage are shown in Fig. 3B. Early T, early trophozoite; Late T, late trophozoite; Schiz, schizont-stage parasites.
[c] GPI (+) indicates GPI-positive and GPI (−) indicates GPI-deficient erythrocytes.
[d] The infection rates are shown in the parenthesis.
[e] Infection rates of GPI-deficient erythrocytes are significantly lower than that of GPI-positive erythrocytes ($P < .01$).

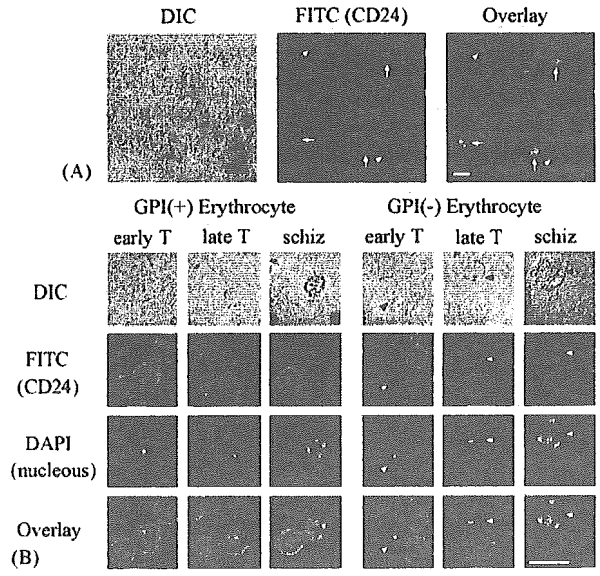

Fig. 3. *P. yoelii* infection of GPI-deficient erythrocytes. Thin blood smears were prepared from a mouse harboring 28% GPI-deficient erythrocytes 3 days after parasite inoculation. Air-dried thin blood smears were fixed with 1% formaldehyde in PBS and GPI-positive erythrocytes were visualized with anti-mouse CD24 antibody and FITC (green). Parasites were visualized with DAPI (blue). Parasites were found in both GPI-positive (arrow) and GPI-deficient (arrow head) erythrocytes (A). In both GPI-positive (arrow) and GPI-deficient (arrow head) erythrocytes, parasites can be matured up to the schizont-stage (B). Scale bar = 5 μm.

tified by DAPI nuclear staining were found in both GPI-positive (Fig. 3A, arrow) and GPI-deficient (Fig. 3A, arrow head) erythrocytes; however, the infection rate in GPI-deficient erythrocytes was only 40–55% that of GPI-positive erythrocytes ($P < .01$; Table 4). The proportion of the various asexual parasite stages were similar between the two erythrocyte populations, defined by the size and the number of nuclei (early trophozoite, late trophozoite, and schizont) as shown in Fig. 3B. This indicated that GPI-deficient erythrocytes were partially resistant to *P. yoelii* infection, whereas subsequent parasite maturation was not affected.

4. Discussion

In this report, we have characterized the binding specificity of the RhopH complex to erythrocytes using the rodent malaria parasite, *P. yoelii*. *Py*RhopH complex binding to erythrocytes was species-specific, observed with mouse but not rabbit or human erythrocytes. Binding is abolished following treatment of erythrocytes with trypsin or chymotrypsin, but not with neuraminidase, suggesting involvement of an erythrocyte non-sialylated protein receptor. Neither GPA nor the DARC, both known *P. falciparum* and *P. vivax* malaria parasite receptors, were found to be major *P. yoelii* RhopH complex receptors using knockout mice harboring targeted disruptions of these gene loci. However, we found undetectable *Py*RhopH complex binding and significant reduction of the *P. yoelii* infection of the GPI-deficient erythrocytes. These results indicate that the major erythrocyte receptor for *Py*RhopH complex is a protein, directly or indirectly, attached to the erythrocyte surface via GPI-anchor and that GPI-deficient erythrocytes are resistant to *P. yoelii* infection.

The *P. yoelii* RhopH complex retains erythrocyte-binding activity following a facile freeze-thaw extraction from parasite pellets. This activity forms the basis of a simple, reproducible flow cytometry assay allowing us to characterize the binding of RhopH complexes to control and specific protein-deficient erythrocytes surfaces. A single reaction requires only 1 μl of packed erythrocytes, containing approximately 1×10^7 erythrocytes, far less than the 50 μl of packed erythrocytes required by a classical erythrocyte binding assay using density centrifugation through silicon oil [21]. Furthermore, flow cytometry gating discriminates the major erythrocyte population and thereby minimizes pseudopositive results typically observed due to carry-over of contaminating parasite proteins in the silicon oil-based assay [22]. Using the flow cytometric method we show that binding to mouse erythrocytes increased in a dose-dependent manner, indicating that this method assays binding in a semi-quantitative fashion. Saturation of the binding was not observed using up to 100 μl extract, which was the maximum amount used in this assay (not shown). Attempts to purify intact *Py*RhopH complex having a binding ability have been unsuccessful in our hands. However, the lack of binding of control recombinant protein introduced into parasite extracts indicates *Py*RhopH binding to mouse erythrocytes is a specific interaction.

We propose two possible models for RhopH complex function, based on *Py*RhopH binding to the GPI-anchored receptor. First, the parasite may stimulate recruitment of cholesterol-rich lipid micromembrane domains around the erythrocyte surface entry point via synapse formation of GPI-anchored proteins with the RhopH complex. In accordance with this model, RhopH complex proteins were observed to be released onto the erythrocyte surface following merozoite contact with erythrocytes [11]. Second, because GPI-anchored proteins are recruited into the parasitophorous vacuole membrane during vacuole formation [1] and the RhopH complex is mainly released into the vacuole [11], it is conceivable that the RhopH complex functions in the parasitophorous vacuole by interacting with erythrocyte molecules that are recruited into the PVM. Recently a RhopH complex component was detected on the erythrocyte cytosol side of the PVM in *P. falciparum* [23]. Although the mechanisms of RhopH complex translocation from the parasite- to erythrocyte cytosol-aspect of the PVM are still unknown, the RhopH complex binding to the membrane component may be linked to this process.

We found that GPI-deficient mouse erythrocytes were partially resistant to *P. yoelii* infection. Because GPI-deficient erythrocytes appear to support normal growth of *P. yoelii*, once infected, the low infectivity of *P. yoelii* to the GPI-deficient erythrocytes indicates that impairment occurs early in the asexual blood stage cycle. Thus we propose that the in-

fection resistance is due to refractory invasion, probably due to impairment of the interaction between the parasite ligand and the erythrocyte receptor. It is formally possible that the GPI-deficient erythrocytes are refractory to invasion due to a decrease in their "deformability"; however, we feel that this explanation is unlikely, because *P. falciparum* parasites efficiently invade and grow normally within GPI-deficient erythrocytes obtained from paroxysmal nocturnal hemoglobinuria patients [24,25].

What is the difference in the invasion efficiency of *P. yoelii* and *P. falciparum* parasites to GPI-deficient erythrocytes? Although, it is plausible that the RhopH complex binding does not serve an essential biological role in invasion and solely mediates increased invasion efficiency, if the resistance of the *P. yoelii* infection to the GPI-deficient erythrocyte were due to abolished or reduced *Py*RhopH complex binding, then the normal infection of GPI-deficient erythrocytes by *P. falciparum* might be explained as follows. First, it might be proposed that the *Pf*RhopH complex receptor is not a GPI-anchored erythrocyte surface protein. Second, because RhopH1, one of the components of the RhopH complex, is encoded by a multigene family consisting of at least five paralogous members in *P. falciparum*, it is plausible that *Pf*RhopH1 determines receptor specificity and that multiple *Pf*RhopH1 recognize non-GPI-anchored proteins. From this point of view, *pyrhoph1ap*, a *pyrhoph1a* paralog encoding *Py*RhopH1, may explain partial but not complete resistance of the GPI-deficient erythrocytes to the *P. yoelii* infection. Such findings of multiple invasion pathways are well documented for the *Plasmodium dbl-ebp* gene family [26]. For example, *P. vivax* cannot invade erythrocytes lacking DARC, the receptor for the *P. vivax* Duffy binding protein (*Pv*DBP), a *P. vivax dbl-ebp* gene product. However, EBA-175, one of the *P. falciparum dbl-ebp* gene products, binds GPA, but *P. falciparum* can efficiently invade GPA-deficient erythrocytes. This might be explained by the paralogous gene products of EBA-175, such as BAEBL and JESEBL, which bind proteins other than GPA on the erythrocyte surface [27,28].

It is of interest to determine if erythrocyte GPI-anchored proteins are involved in human malaria parasite erythrocyte invasion, such as decay-accelerating factor (DAF, CD55; bearing Cromer blood group), Dombrock (Do) glycoprotein (Dombrock blood group) and acetylcholinesterase (Cartwright blood group). It should be also noted that GPI-anchored proteins may play important roles for the host cell invasion by other members of the apicomplexa such as *Toxoplasma gondii*, which is known to recruit GPI-anchored-proteins into the PVM [29].

Acknowledgements

We thank K. Kameda (INCS, Ehime University) for helping with the flow cytometry analysis. We also thank T.J. Templeton (Weill Medical College of Cornell University) for critical reading of the manuscript. Animal experiments in this study were carried out in compliance with the Guide for Animal Experimentation at Ehime University School of Medicine. This work was supported by grants from the Ministry of Education, Culture, Sports, Science and Technology, Japan (14370084 and 15406015 to M.T.; 15790215 to O.K.).

References

[1] Lauer S, VanWye J, Harrison T, et al. Vacuolar uptake of host components, and a role for cholesterol and sphingomyelin in malarial infection. EMBO J 2000;19:3556–64.
[2] Campbell GH, Miller LH, Hudson D, Franco EL, Andrysiak PM. Monoclonal antibody characterization of *Plasmodium falciparum* antigens. Am J Trop Med Hyg 1984;33:1051–4.
[3] Holder AA, Freeman RR, Uni S, Aikawa M. Isolation of a *Plasmodium falciparum* rhoptry protein. Mol Biochem Parasitol 1985;14:293–303.
[4] Lustigman S, Anders RF, Brown GV, Coppel RL. A component of an antigenic rhoptry complex of *Plasmodium falciparum* is modified after merozoite invasion. Mol Biochem Parasitol 1988;30:217–24.
[5] Hienne R, Ricard G, Fusaï T, et al. *Plasmodium yoelii*: Identification of rhoptry proteins using monoclonal antibodies. Exp Parasitol 1998;90:230–5.
[6] Brown HJ, Coppel RL. Primary structure of a *Plasmodium falciparum* rhoptry antigen. Mol Biochem Parasitol 1991;49:99–110.
[7] Shirano M, Tsuboi T, Kaneko O, Tachibana M, Adams JH, Torii M. Conserved regions of the *Plasmodium yoelii* rhoptry protein RhopH3 revealed by comparison with the *P. falciparum* homologue. Mol Biochem Parasitol 2001;112:297–9.
[8] Kaneko O, Tsuboi T, Ling IT, et al. The high molecular mass rhoptry protein, RhopH1, is encoded by members of the *clag* multigene family in *Plasmodium falciparum* and *Plasmodium yoelii*. Mol Biochem Parasitol 2001;118:237–45.
[9] Ling IT, Kaneko O, Narum DL, et al. Characterization of the *rhoph2* gene of *Plasmodium falciparum* and *Plasmodium yoelii*. Mol Biochem Parasitol 2003;127:47–57.
[10] Ling IT, Florens L, Dluzewski AR, et al. The *Plasmodium falciparum clag9* gene encodes a rhoptry protein that is transferred to the host erythrocyte upon invasion. Mol Microbiol 2004;52:107–18.
[11] Sam-Yellowe TY, Shio H, Perkins ME. Secretion of *Plasmodium falciparum* rhoptry protein into the plasma membrane of host erythrocytes. J Cell Biol 1988;106:1507–13.
[12] Sam-Yellowe TY, Perkins ME. Interaction of the 140/130/110 kDa rhoptry protein complex of *Plasmodium falciparum* with the erythrocyte membrane and the liposomes. Exp Parasitol 1991;73:161–71.
[13] Siddiqui WA, Tam LQ, Kramer KJ, et al. Merozoite surface coat precursor protein completely protects *Aotus* monkeys against *Plasmodium falciparum* malaria. Proc Natl Acad Sci USA 1987;84:3014–8.
[14] Cooper JA, Ingram LT, Bushell GR, et al. The 140/130/105 kilodalton protein complex in the rhoptries of *Plasmodium falciparum* consists of discrete polypeptides. Mol Biochem Parasitol 1988;29:251–60.
[15] Doury JC, Bonnefoy S, Roger N, Dubremetz JF, Mercereau-Puijalon O. Analysis of the high molecular weight rhoptry complex of *Plasmodium falciparum* using monoclonal antibodies. Parasitology 1994;108:269–80.
[16] Cowman AF, Baldi DL, Healer J, et al. Functional analysis of proteins involved in *Plasmodium falciparum* merozoite invasion of red blood cells. FEBS Lett 2000;476:84–8.
[17] Tsuboi T, Cao YM, Hitsumoto Y, Yanagi T, Kanbara H, Torii M. Two antigens on zygotes and ookinetes of *Plasmodium yoelii* and *Plasmodium berghei* that are distinct targets of transmission-blocking immunity. Infect Immun 1997;65:2260–4.

[18] Fukuma N, Akimitsu N, Hamamoto H, Kusuhara H, Sugiyama Y, Sekimizu K. A role of the Duffy antigen for the maintenance of plasma chemokine concentrations. Biochem Biophys Res Commun 2003;303:137–9.
[19] Arimitsu N, Akimitsu N, Kotani N, et al. Glycophorin A requirement for expression of O-linked antigens on the erythrocyte membrane. Genes Cells 2003;8:769–77.
[20] Murakami Y, Kinoshita T, Maeda Y, Nakano T, Kosaka H, Takeda J. Different roles of glycosylphosphatidylinositol in various hematopoietic cells as revealed by a mouse model of paroxysmal nocturnal hemoglobinuria. Blood 1999;94:2963–70.
[21] Klotz FW, Orlandi PA, Reuter G, et al. Binding of *Plasmodium falciparum* 175-kilodalton erythrocytes binding antigen and invasion of murine erythrocytes requires *N*-acetylneuraminic acid but not its O-acetylated form. Mol Biochem Parasitol 1992;51:49–54.
[22] Lobo CA, Rodriguez M, Reid M, Lustigman S. Glycophorin C is the receptor for the *Plasmodium falciparum* erythrocyte binding ligand PfEBP-2 (baebl). Blood 2003;101:4628–31.
[23] Hiller NL, Akompong T, Morrow JS, Holder AA, Haldar K. Identification of a stomatin orthologue in vacuoles induced in human erythrocytes by malaria parasites. A role for microbial raft proteins in apicomplexan vacuole biogenesis. J Biol Chem 2003;278: 48413–21.
[24] Soubes SC, Reid ME, Kaneko O, Miller LH. Search for the sialic acid-independent receptor on red blood cells for invasion by *Plasmodium falciparum*. Vox Sang 1999;76:107–14.
[25] Pattanapanyasat K, Walsh DS, Yongvanitchit K, Wattanasakul N, Wanachiwanawin W, Webster KH. Robust in vitro replication of *Plasmodium falciparum* in glycosyl-phosphatidylinositol-anchored membrane glycoprotein-deficient red blood cells. Am J Trop Med Hyg 2003;69:360–5.
[26] Adams JH, Kaneko O, Blair PL, Peterson DS. An expanding *ebl* family of *Plasmodium falciparum*. Trends Parasitol 2001;17:297–9.
[27] Mayer DC, Kaneko O, Hudson-Taylor DE, Reid ME, Miller LH. Characterization of a *Plasmodium falciparum* erythrocyte-binding protein paralogous to EBA-175. Proc Natl Acad Sci USA 2001;98:5222–7.
[28] Gilberger TW, Thompson JK, Triglia T, Good RT, Duraisingh MT, Cowman AF. A novel erythrocyte binding antigen-175 paralogue from *Plasmodium falciparum* defines a new trypsin-resistant receptor on human erythrocytes. J Biol Chem 2003;278:14480–6.
[29] Mordue DG, Desai N, Dustin M, Sibley LD. Invasion by *Toxoplasma gondii* establishes a moving junction that selectively excludes host cell plasma membrane proteins on the basis of their membrane anchoring. J Exp Med 1999;190:1783–92.

Available online at www.sciencedirect.com
SCIENCE DIRECT®
ELSEVIER
Molecular & Biochemical Parasitology 143 (2005) 20–28
MOLECULAR & BIOCHEMICAL PARASITOLOGY

Apical expression of three RhopH1/Clag proteins as components of the *Plasmodium falciparum* RhopH complex☆

Osamu Kaneko[a,*], Brian Y.S. Yim Lim[b], Hideyuki Iriko[a], Irene T. Ling[b], Hitoshi Otsuki[a], Munira Grainger[b], Takafumi Tsuboi[c], John H. Adams[d], Denise Mattei[e], Anthony A. Holder[b], Motomi Torii[a]

[a] *Department of Molecular Parasitology, Ehime University School of Medicine, Toon, Shigenobu-cho, Ehime 791-0295, Japan*
[b] *Division of Parasitology, MRC National Institute for Medical Research, The Ridgeway, Mill Hill, London NW7 1AA, UK*
[c] *Cell-Free Science and Technology Research Center, Ehime University, Matsuyama, Ehime 790-8577, Japan*
[d] *Department of Biological Sciences, University of Notre Dame, Notre Dame, Indiana 46556, USA*
[e] *Institut Pasteur, Biology of Host Parasite Interactions, URA 2581, F-75724, Paris CEDEX 15, France*

Received 25 January 2005; received in revised form 28 April 2005; accepted 2 May 2005
Available online 31 May 2005

Abstract

The *Plasmodium falciparum* high molecular mass rhoptry protein ('PfRhopH') complex is important for parasite growth and comprises three distinct gene products: RhopH1, RhopH2 and RhopH3. We have previously shown that *P. falciparum* RhopH1 is encoded by either PFC0110w (*clag3.2*) or PFC0120w (*clag3.1*), members of the previously-named *clag* (cytoadherence-linked asexual gene) multigene family. In this report, we have further characterized *rhoph1/clag* members in terms of gene structure, transcription and protein expression. The cDNA sequences for all five *rhoph1/clag* members were determined, confirming previous in silico predictions of intron–exon boundaries. All member genes were transcribed in HB3 and 3D7 parasite lines, but *clag3.2* was not transcribed in Dd2 parasites. The peak abundance of transcripts for all genes was observed during the late schizont stage. Antisera specific to Clag2 and Clag3.1 localized these proteins to the apical end of merozoites in segmented schizonts, and both proteins are found to be components of the PfRhopH complex. PfRhopH complex that was immunoprecipitated with *anti*-Clag9 antibody contained neither Clag2 nor Clag3.1, thereby suggesting that PfRhopH complexes contain only individual *rhoph1/clag* gene products. Since the PfRhopH complex binds the erythrocyte surface, and RhopH2 and RhopH3 are encoded by single copy genes, the RhopH1/Clag proteins may serve to confer some degree of specificity to the roles of the individual complexes.
© 2005 Elsevier B.V. All rights reserved.

Keywords: Clag; Cytoadherence; Invasion; Malaria; Merozoite; Rhoptry

1. Introduction

Plasmodium species are obligate intracellular parasites and entry into host erythrocytes is a prerequisite for the development of asexual stages. *Plasmodium* merozoites discharge the contents of their apical organelles (micronemes, rhoptries, dense granules) during the invasion process. The molecules contained within these organelles, including erythrocyte binding proteins, are considered important for erythrocyte invasion and have been studied as vaccine targets with the aim of inducing antibodies to block invasion. For example, passive immunization with monoclonal antibodies specific for a 235-kDa erythrocyte binding protein in the rhoptry [1], or active immunization with the protein [2], protects mice against blood stage challenge with *Plasmodium yoelii*. Other erythrocyte binding molecules within rhoptries are in a complex of high molecular mass proteins (the

Abbreviations: aa, amino acid(s); cDNA, complementary DNA; clag, cytoadherence-linked asexual gene; gDNA, genomic DNA; nt, nucleotide(s); PCR, polymerase chain reaction; PBS, phosphate buffered saline; SSU rRNA, small subunit ribosomal RNA

☆ *Note:* Nucleotide sequence data reported in this paper are available in the GenBank™, EMBL, and DDBJ databases under the accession numbers: AB193597–AB193601.

* Corresponding author. Tel.: +81 89 960 5286; fax: +81 89 960 5287.
E-mail address: okaneko@m.ehime-u.ac.jp (O. Kaneko).

0166-6851/$ – see front matter © 2005 Elsevier B.V. All rights reserved.
doi:10.1016/j.molbiopara.2005.05.003

RhopH complex) comprised of three distinct polypeptides: RhopH1, RhopH2 and RhopH3 that are encoded by unrelated genes [3–6]. Antibodies against the *P. falciparum* RhopH (PfRhopH) complex partially inhibit growth of *P. falciparum* in vitro and in vivo, consistent with its potential as a vaccine target [7–9]. The PfRhopH complex binds the erythrocyte and distributes into the erythrocyte and parasitophorous vacuolar membranes [10,11], and has been detected in ring-stage parasites [5,12,13], indicating an important role during the establishment of the parasitophorous vacuole. The importance of the complex has further been emphasized by the failure of attempts to disrupt the *pfrhoph3* gene locus, suggesting that the gene is necessary for parasite survival [14].

The genes encoding RhopH3 in *P. falciparum* and *P. yoelii* were identified some years ago [15,16]. Detailed molecular and functional analysis of other members of the RhopH complex was hindered until the recent identification of the genes encoding RhopH1 and RhopH2 in *P. falciparum* and *P. yoelii* [13,17]. Interestingly, we found by MALDI-ToF analysis that *P. falciparum* RhopH1 was encoded by either PFC0110w (*clag3.2*) or PFC0120w (*clag3.1*) [17]. These two genes are members of a family originally defined by a cytoadherence-linked asexual gene on chromosome 9 (*clag9*) [18,19]. Although the *clag9* gene product was originally proposed to mediate cytoadhesion between host endothelial cells and the surface of infected erythrocytes, we have shown by immunoelectron microscopy and immunochemical means that Clag9 is actually located within the rhoptry bodies in the (developing) merozoite, and is a component of the RhopH complex [20]. Based on this association, we renamed the '*clag*' multigene family '*rhoph1/clag*' [17]. This work raises the possibility that other *rhoph1/clag* gene products are also components of the PfRhopH complex. With the exception of Clag9, the gene structure (including intron–exon boundaries), transcription and protein expression profiles of other RhopH1/Clag members have yet to be fully characterized.

In this paper we address the unresolved issues of gene structure, transcription and translation and determine the phylogenetic relationship of all known *rhoph1/clag* gene products. In addition, using specific antisera we demonstrate the apical localization of Clag2 and Clag3.1, and determine their associations with the PfRhopH complex.

2. Materials and methods

2.1. Parasite lines

The 3D7, HB3, and Dd2 cloned lines of *P. falciparum* and 20 progeny between HB3 and Dd2, 1BB5, 3BA6, 3BD5, B1SD, B4R3, GC03, GC06, QC01, QC13, QC23, QC34, SC01, SC05, TC05, TC08, C188, C408, Ch3-116, Ch3-61, and D43 (kind gift from Dr. Wellems, NIH) [21] were maintained in vitro, essentially as previously described [22].

2.2. DNA and RNA isolation

Genomic DNA (gDNA) was isolated from *P. falciparum* using IsoQuick™ (Orca Research Inc., Bothell, WA). To obtain complementary DNA (cDNA), parasites at the schizont-stage were purified by differential centrifugation on a 70/40% Percoll-sorbitol gradient. To determine transcription throughout the asexual stages, parasites were synchronized using a MACS Type-D depletion column in conjunction with a SuperMACS II magnetic separator (Miltenyi Biotec GmbH, Germany) [13,23,24]. Schizonts were purified by passing a culture through the magnetized column, after which released merozoites were allowed to invade uninfected erythrocytes for 4 h before the removal of all remaining schizonts using the magnet. Part of the culture was harvested immediately and every 6 h thereafter. Total RNA was isolated from parasite-infected erythrocytes stored at −20 °C in RNA*later*™ (Qiagen, Valencia, CA), using the RNeasy Mini Kit (Qiagen). Following DNase treatment, cDNA was generated with random hexamers using an Omniscript Reverse Transcription Kit (Qiagen).

2.3. Identification of the chromosomal location of clagb1

Oligonucleotides were designed to differentiate between the *clagb1* genes of HB3 and Dd2 parasite lines. These were based on preliminary sequence data from the two lines (data not shown). Specific DNA fragments were PCR-amplified using 5′-GCTTATAATATAAAAATTCACGTTTTCG-3′ (common) and 5′-AAGTTCAACAAGTAATCATTTTAGTGG-3′ (specific for HB3) or 5′-ATAGGTAAAACAAGTACTTATATTAAATC-3′ (specific for Dd2). PCR amplification was performed for 20 progeny between HB3 and Dd2, and the inheritance pattern was compared with the segregation table [25].

2.4. Quantification of rhoph1/clag transcripts

Transcription of all five members of the *rhoph1/clag* family was evaluated in the HB3 parasite lines by real-time reverse transcription (RT)-PCR using the QuantiTect SYBR Green PCR Kit (Qiagen) and the LightCycler System (Roche). As a positive control, the gene for the asexual-type small subunit ribosomal RNA (A-Type SSU rRNA) was also evaluated. Oligonucleotides used are detailed in Table 1. The same oligonucleotides were used in the PCR amplification of 3D7 parasite line cDNA, generating DNA fragments, which were ligated into the pGEM-T Easy® plasmid (Promega, Madison, WI), and used in the production of a standard curve to evaluate the copy number of each transcript.

2.5. Recombinant protein expression

DNA fragments encoding N-terminal sequences specific to each of the RhopH1/Clag members were PCR-amplified

Table 1
Oligonucleotides used in the quantitative real-time RT-PCR of *pfrhoph1/clag* genes

Target gene	Oligonucleotide sequence
clag2	5′-TCATCACATAATTATTTCCTACATGAG-3′ 5′-TAATCTTGATATATATCTAAGGTTTTCAT-3′
clag3.1	5′-GGAGAAACACTTATATTAGGCGATAA-3′ 5′-TAATTTTTTAGTGCTAATTTTAATACGGT-3′
clag3.2	5′-GGAGAAACACTTATATTAGGCGATAA-3′ 5′-GTAATTTTTTAGTGCTAATTTTAATACAAC-3′
clag8	5′-CCCTTAGATAGTAATTTTATGAATGAAG-3′ 5′-TAATCTTGATAAATATCTAATGTTCTAAC-3′
clag9	5′-TAAAAGAAGTGGTAAATGATTTTTTTGTT-3′ 5′-CTTTCTCTCTATCTGCTTGGCTCAT-3′
SSU rRNA[a]	5′-ACGATCAGATACCGTCGTAATCTT-3′ 5′-CAATCTAAAAGTCACCTCGAAAGATG-3′

[a] Oligonucleotides previously detailed [26].

from *P. falciparum* HB3 gDNA and ligated into the pGEM-T Easy® plasmid. Inserts were digested with *Nhe*I and *Bam*HI, and ligated into the pJWE2 plasmid, yielding pCL2, pCL3.1, pCL3.2, pCL8, and pCL9 for DNA immunization [27,28]. Oligonucleotides used in the PCR amplification are detailed in Table 2. Recombinant proteins corresponding to the region used in the DNA immunization (Fig. 1) were produced in *E. coli* with the pET32b system (Novagen, Madison, WI) by ligating inserts into *Eco*RV site, yielding rCL2N, rCL3.1N, rCL3.2N, rCL8N, and rCL9N. Expressed recombinant proteins were detected using an *anti*-penta-His antibody (Qiagen) by Western blot analysis.

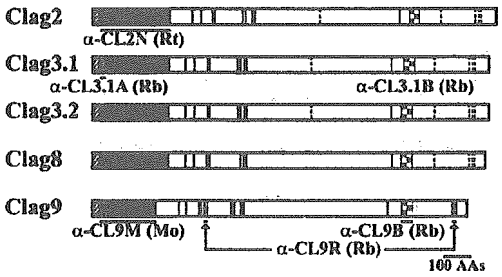

Fig. 1. Schematic illustrating the individual *Plasmodium falciparum* RhopH1/Clag family members showing the regions used in the generation of specific antisera. Shading indicates putative signal peptide sequences. Solid vertical lines indicate cysteine residues conserved throughout the multigene family, broken lines indicate those conserved in-part. Colored boxes illustrate regions used in the generation of specific sera: rabbit *anti*-Clag3.1 MAP-peptide serum A (α-CL3.1A) and rabbit *anti*-Clag9 peptides (α-CL9R) in solid green; rat *anti*-Clag2 DNA immunization serum (α-CL2N) and mouse *anti*-Clag9 DNA immunization serum (α-CL9M) in solid red; rabbit *anti*-Clag3.1 serum B (α-CL3.1B) and *anti*-Clag9 serum B (α-CL9B) in checkered red. Regions used only to check antibody specificity are in blue.

2.6. Production of RhopH1/Clag-specific antisera

DBA/2 mice and Wistar rats were immunized by intradermal injection in the ear pinna with 50 or 500 μg plasmid, four times at 3 week intervals, generating antisera α-CL2N, α-CL3.1N, α-CL3.2N, α-CL8N, and α-CL9N. Rabbit *anti*-CL3.1A serum was generated with MAP-peptide (NQNENDTISQNVNQH) corresponding to amino acid (aa) position 29–43 of Clag3.1. Rabbit *anti*-CL3.1B

Table 2
Oligonucleotides used in the production of PfRhopH1/Clag DNA immunization constructs and recombinant proteins

Protein (amino acid position)	Name	Oligonucleotide sequence[a]
Clag2 (25–271)	pCL2	5′-GCTAGCTCTATAAATGATAATGTAAATGAAAA-3′ 5′-CTCGAGGTGTGCATCCATTATTTCAATTT-3′
	rCL2N	5′-TTCTATAAATGATAATGTAAATGAAA-3′ 5′-TCGTGTGCATCCATTATTTCAA-3′
Clag3.1 (25–249)	pCL3.1	5′-GCTAGCTCAATAAATGAAAATCAAAATGAAAA-3′ 5′-CTCGAGATCGTTTGAATTCATTACATCTATTTTA-3′
	rCL3.1N	5′-TTCAATAAATGAAAATCAAAATGAAA-3′ 5′-TCGTTTGAATTCATTACATCTATT-3′
Clag3.2 (25–251)	pCL3.2	5′-GCTAGCTCAATAAATGAAAATGAAAATTTAGG-3′ 5′-CTCGAGGTTTGAATTCATTACATCTATTTTA-3′
	rCL3.2N	5′-TTCAATAAATGAAAATGAAAATTTAG-3′ 5′-TCGTTTGAATTCATTACATCTATT-3′
Clag8 (25–240)	pCL8	5′-GCTAGCTCCATTAATGAGAGTAAAAATGTGAATG-3′ 5′-CTCGAGATTTGTACTCATTAGATCTATTTTAGTAT-3′
	rCL8N	5′-TTCCATTAATGAGAGTAAAAATGT-3′ 5′-TCATTTGTACTCATTAGATCTATT-3′
Clag9 (24–222)	pCL9	5′-GCTAGCACCTACAAAGGAGATAATATAAAT-3′ 5′-CTCGAGATCATAATCAATTATATCAGATTTC-3′
	rCL9N	5′-TACCTACAAAGGAGATAATATAAA-3′ 5′-TCATCATAATCAATTATATCAGATT-3′

[a] *Nhe*I and *Bam*HI, restriction sites are underlined.

and *anti*-CL9B sera were generated by immunization with KLH-conjugated synthetic peptides (CSGYKSPESFFF and CKARTEGIIGKEWYK, respectively). Target regions used in the generation of the specific antisera are outlined in Fig. 1. The rabbit antiserum and mouse monoclonal antibody mAb 61.3 against PfRhopH2 and rabbit *anti*-Clag9 (α-CL9R) have been described previously [4,20]. Mouse *anti*-SERA5 (α-SE47′) was a kind gift from T. Horii at Osaka University [29].

2.7. SDS-PAGE and western blot analysis

SDS-extracted proteins from *P. falciparum* or recombinant proteins were dissolved in SDS-PAGE loading buffer, incubated at 100 °C for 3 min, and subjected to electrophoresis on a 5–20% polyacrylamide gel (ATTO, Japan). Proteins were then transferred to a 0.22 μm PVDF membrane (Bio-Rad, Hercules, CA). The proteins were immunostained with antisera followed by horseradish peroxidase-conjugated secondary antibody (Biosource Int., Camarillo, CA) and visualized with ECL Plus (Amersham Biosciences) on RX-U film (Fuji, Japan). The relative molecular sizes of the parasite-encoded proteins were calculated by reference to molecular size standards (BioRad).

2.8. Immunofluorescence microscopy

Thin smears of schizont-enriched *P. falciparum*-infected erythrocytes (Dd2) were prepared on glass slides and stored at −20 °C or −80 °C. The smears were thawed, acetone-fixed, and preincubated with PBS containing 5% non-fat milk at 37 °C for 30 min. They were then incubated with *anti*-RhopH1/Clag antisera at 37 °C for 1 h, followed by fluorescein isothiocyanate (FITC)-conjugated goat *anti*-(IgG and IgM) secondary antibody (Jackson ImmunoResearch Laboratories, West Grove, PA) and Alexa546-conjugated goat *anti*-(IgG and IgM) secondary antibody (Molecular Probes, Eugene, OR) at 37 °C for 30 min. High resolution image-capture and processing were performed using a fluorescence microscope (BX50; Olympus, Japan) and digital camera (IM500; Leica, Germany). 3D7 parasite samples were treated in a similar manner, with the exception of the blocking step, which was performed using PBS with 1% BSA. Clag3.1 and RhopH2 were visualized using rabbit *anti*-CL3.1B and mAb 61.3 followed by incubation with FITC-conjugated *anti*-rabbit IgG antibody (Sigma, Poole, UK) and Texas Red-conjugated *anti*-mouse IgG antibody (Sigma), respectively. Nuclei were stained with 4′,6-diamidino-2-phenylindole (DAPI) or Hoechst-33342 (Sigma). Slides were mounted in CitiFluor glycerol/PBS solution (CitiFluor Ltd, London, UK) and viewed under oil-immersion. Slides were examined using a DeltaVision cooled CCD Imaging System (Applied Precision LLC, Issaquah, WA). Images were analyzed using SoftWoRx, and processed in Adobe Photoshop (Adobe Systems Inc., San José, CA).

2.9. Phylogenetic analysis

To better understand the relationship amongst members of the *P. falciparum rhoph1/clag* multigene family, *Plasmodium vivax* homologs were WU-BLAST-searched (Gish, W. (1996–2004)) in the Institute for Genomic Research website (http://blast.wustl.edu) using amino acid sequences as a query. Deduced amino acid sequences of the first and last exons were used for phylogenetic analysis, since they are comparatively the largest (first exon 258–307 aa; last exon 427–494 aa). Unrooted trees were constructed using the CLUSTAL W algorithm and the Neighbor-Joining method using Kimura's Correction accompanied by Bootstrap Analysis with 1000 replicates [30–32]. The phylogenetic tree was constructed using TreeView [33].

3. Results

3.1. clagb1 is located on chromosome 8

We determined the chromosomal location of *clagb1* (also known as *clagBlob*, *clagb* or *clag7* due to initial assignments and preliminary annotations by the *P. falciparum* Genome Sequencing Project) by linkage analysis of 20 HB3 × Dd2 genetic-cross progeny [23], using nucleotide substitutions of *clagb*1 between HB3 and Dd2 lines as genotypic markers. The inheritance pattern was matched with the HRPII locus on the subtelomeric region of chromosome 8 (data not shown), hence we designate *clagb1* as *clag8* in this report.

3.2. RhopH1/Clag family members can be divided into two subgroups

The cDNA sequences of *clag2*, *-3.1*, and *-8* of Dd2 and *clag3.2* of HB3 were determined (accession numbers AB193597–AB193601) and the actual intron–exon boundaries confirmed the predictions by computer algorithm [17]. WU-BLAST search of the *P. vivax* database (The Institute for Genomic Research website at http://www.tigr.org) revealed three paralogous genes with accession numbers 1047, 3844, and 3944, respectively named as *pvrhoph1_1047*, *_3844*, and *_3944* in this report. Intron-exon boundaries were confirmed for the first and last introns of *pvrhoph1_1047* and *_3944* by sequencing RT-PCR products from *P. vivax* field isolates; the first and last exon sequences were used in the analysis. As the RT-PCR products for *pvrhoph1_3844* were not amplified, this gene was excluded from the analysis. The length of the deduced amino acid sequences of the first exons were 264 and 258 aa, and for the last exons 501 and 428 aa, for PvRhopH1_1047 and _3944, respectively. Using deduced amino acid sequences from five *P. falciparum* (3D7 line), two *P. yoelii* (17XL strain), and two *P. vivax* (SalI strain) homologs, the phylogenetic relationship amongst *Plasmodium* RhopH1/Clag family members was

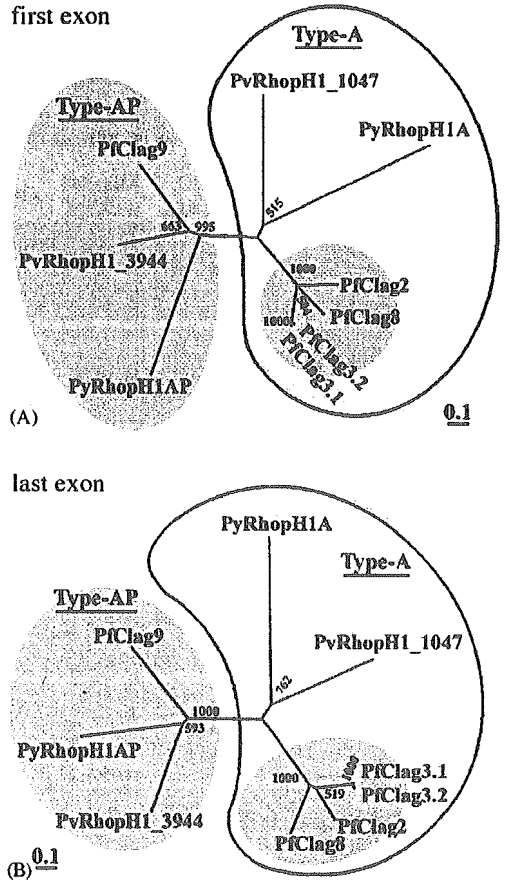

Fig. 2. Phylogenetic relationship between *Plasmodium* RhopH1/Clag proteins based on the deduced amino acid sequences of the first exon (Panel A) or last exon (Panel B) for *P. falciparum* (5 paralogs), *Plasmodium yoelii* (2 paralogs), and *Plasmodium vivax* (2 paralogs). Unrooted phylogenetic trees were constructed using the CLUSTAL W algorithm and the Neighbor-Joining method, using Kimura's Correction accompanied by Bootstrap Analysis with 1000 replicates. The number of amino acid substitutions per site of 0.1 is indicated. Groups differentiated from other proteins with the bootstrap values above 90% are masked. RhopH1/Clag family members were subdivided into two groups, Type-A and -AP, which are indicated on the tree.

analyzed (Fig. 2). Two unrooted phylogenetic trees imply the following. Clag9, PyRhopH1A-P, and PvRhopH1_3944 form a single group designated Type-AP, indicating that these three orthologs shared an ancestral gene, which had diversified from other RhopH1/Clag members before speciation in the *Plasmodium* genus occurred. RhopH1/Clag members can therefore be divided into two subgroups, Type-AP (as above) and Type-A that contains the remaining members. Additionally, the *P. falciparum* Type-A RhopH1/Clag group contains four paralogous members, implying the continued evolution of this subgroup. Preliminary analysis indicates that the remaining *P. vivax rhoph1* member, *pvrhoph1_3844*, belongs to the Type-A subgroup, also supporting the continued evolution of this subgroup (data not shown).

3.3. All five members of the pfrhoph1/clag multigene family are transcribed

RT-PCR amplifications using oligonucleotide sets specific for each *rhoph1/clag* family member in HB3, Dd2, and 3D7 parasite lines detected transcripts of all members, with the exception of *clag3.2* in Dd2 (data not shown). Thus, parasites have the ability to transcribe all five members.

To determine the transcription pattern through the asexual stages of the parasite life-cycle, quantitative RT-PCR was performed on the HB3 parasite line prepared from a synchronized culture harvested at 6 h intervals. Transcription was seen to peak for all members around 42–46 h after invasion, when parasites were in the schizont stage (Fig. 3). However, an earlier elevation in the number of *clag9* transcripts was observed at 36–40 h (6 h before the maximal peak), when the level of transcription of *clag9* was approximately 15% of its maximum, whilst that for other members was 0–5%. Transcriptome data compiled in the PlasmoDB web site [34,35] also indicated an earlier elevation of *clag9* transcripts compared with those of *clag2*, *-3.1*, and *-3.2*. Similar results showing a peak in transcription for all genes around 35–44 h post-invasion were observed in RT-PCR studies of *P. falciparum* 3D7 parasites prepared from a synchronized culture harvested at 3 h intervals (data not shown).

3.4. Production of antisera specific to Clag2, -3.1 and -9

Antisera were generated by DNA immunization using sequences selected from the N-terminal end of five RhopH1/Clag members and their specificity evaluated using *E. coli*-expressed recombinant protein. We found that the rat *anti*-Clag2 serum and mouse *anti*-Clag9 serum did not cross react with other members (Fig. 4A). Other antisera generated

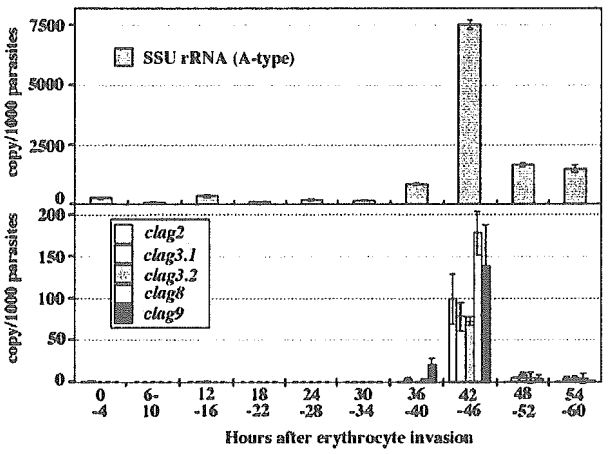

Fig. 3. Transcriptional analysis by quantitative RT-PCR of *rhoph1/clag* genes throughout the asexual blood stages of the *P. falciparum* (HB3 line) life-cycle. *Y*-axis indicates copy number of each transcript detected per 1000 parasites. Positive detection of the asexual-type small subunit ribosomal RNA (A-Type SSU rRNA) transcripts indicated successful cDNA synthesis. Error bars were generated from duplicates.

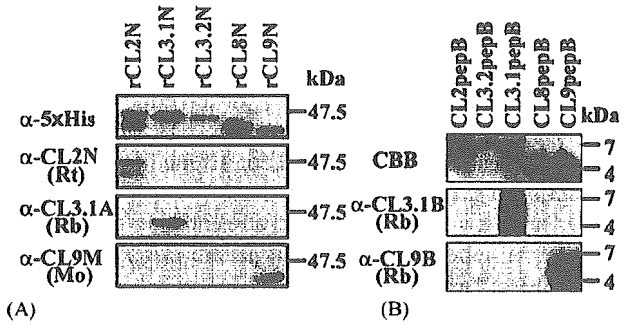

Fig. 4. Specificity of each antiserum against *E. coli*-expressed recombinant proteins for α-CL2N, α-CL3.1A, and α-CL9M (Panel A), and synthetic peptides for α-CL3.1B and α-CL9B (Panel B). CBB denotes Coomassie Brilliant Blue staining of synthetic peptides. The expressed regions of rCL2N, -3.1N, -3.2N, -8N, and -9N are indicated as filled boxes, CL2pepB, -3.1pepB, -3.2pepB, -8pepB, and -9pepB are indicated as checkered boxes in Fig. 1. α-5 × His indicates *anti*-penta His antibody.

in this manner showed cross-reactivity (data not shown), and were omitted from further analysis. The specificity of rabbit *anti*-Clag3.1 peptide serum A was confirmed using the same set of *E. coli*-expressed recombinant proteins (Fig. 4A) and that of rabbit *anti*-Clag3.1 peptide serum B and *anti*-Clag9 peptide serum B with synthetic peptides (Fig. 4B). Only antisera that were specific were used in the following studies.

3.5. Clag2 and -3.1 are expressed at the apical end of merozoites

All specific antisera against Clag members -2, -3.1, and -9 described above were used in indirect immunofluorescence assays (IFA), resulting in a specific reaction at the apical end of the merozoites in schizont-stage parasites. Overlaid images of the double-staining for *anti*-Clag3.1 and *anti*-PfRhopH2 or *anti*-Clag3.1 and *anti*-Clag9 sera reacting with segmented schizonts showed indistinguishable patterns of localization for these proteins (Fig. 5A–B). RhopH2 and Clag9 were previously shown to be located within the rhoptry body by immunoelectron microscopy [18], thus our IFA data suggest that Clag3.1 is localized within the rhoptries of segmented schizonts. Overlaid images of the double-staining for Clag2 and -3.1 also showed an indistinguishable pattern (Fig. 5C), indicating that Clag2 is also localized within the rhoptries of segmented schizonts. All segmented schizont-stage parasites observed by microscopy were positive for each RhopH1/Clag member, indicating that at least three members are co-expressed in all *P. falciparum* merozoites.

3.6. Clag2 and -3.1 are expressed in at least three parasite lines

Western blotting analysis was performed using the specific antisera shown to be reactive by IFA. To develop an appropriately effective extraction method for the RhopH

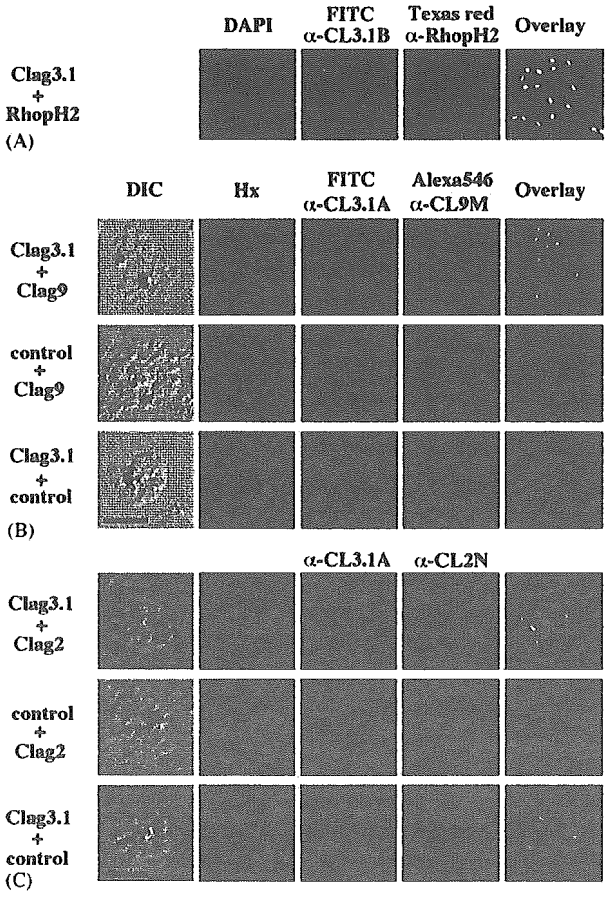

Fig. 5. Apical expression of RhopH1/Clag members -2, -3.1, and -9 in *P. falciparum* segmented schizonts. Schizont-infected erythrocytes were dual-labeled with α-CL3.1B and α-RhopH2 mAb 61.3 in the 3D7 parasite line (Panel A); α-CL3.1A and α-CL9M (Panel B) and α-CL3.1A and α-CL2N (Panel C) in Dd2 parasite line. Overlaid images are shown in the right-hand panels. All segmented schizont-stage parasites are positive for the antisera against Clag2, -3.1, and -9. Nuclei are counterstained with either DAPI or Hoechst-33342 (Hx). Scale bar represents 5 μm.

complex, parasite proteins were sequentially extracted from 3D7 schizont-stage parasites. Proteins were extracted by repeated freeze–thaw cycles in PBS, followed by extraction of the insoluble pellet in 1% Triton X-100. Finally, the Triton-insoluble fraction was dissolved in 2% SDS. The results indicated that most of Clag3.1 is extracted by a simple freeze–thaw step (Fig. 6A). Using the soluble freeze–thaw extract, we examined the protein expression of Clag2 and -3.1 in three parasite lines: 3D7, Dd2, and HB3. Antisera against Clag2 and Clag3.1 produced a specific reaction at approximately 155 kDa in Western Blot analysis of PBS soluble extracts from these three parasite lines (Fig. 6B).

3.7. Clag2 and -3.1 form a complex with RhopH2

We further examined if Clag2 and -3.1 were involved in the RhopH protein complex by Western blot analysis

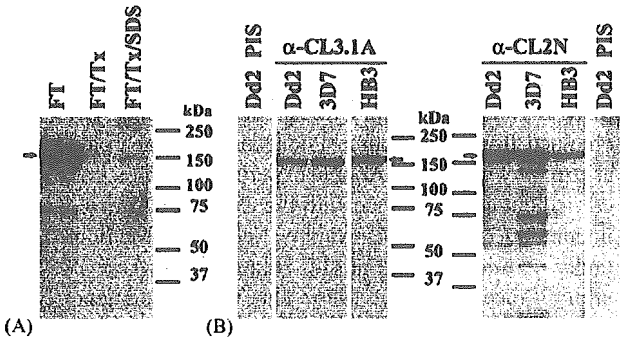

Fig. 6. Western blot analysis with *anti*-Clag2 (α-CL2N) and *anti*-Clag3.1 (α-CL3.1A) sera. (Panel A) Parasite proteins were sequentially extracted by repeated freeze–thaw cycles (FT) followed by 1% Triton X-100 (FT/Tx), then 2% SDS (FT/Tx/SDS) in PBS. Clag3.1 was exclusively detected in the sample extracted by simple freeze–thaw procedure. (Panel B) Clag2 and -3.1 were detected under reducing conditions as ~155 kDa bands in three parasite lines in the freeze–thaw fractions. 'PIS' denotes preimmune serum, which did not give any positive reactivity at 155 kDa when using Dd2 parasites.

of immunoprecipitated RhopH protein. Clag2, -3.1, and -9 were detected in the RhopH complex precipitated using *anti*-RhopH2 antiserum, indicating that these members are components of RhopH complex (Fig. 7). To examine if different RhopH1/Clag members co-exist in a single RhopH complex, the RhopH complex precipitated using *anti*-Clag9 serum was subjected to Western Blotting and the existence of other members of the RhopH1/Clag family was evaluated by probing with the specific antisera (Fig. 7). In this complex, RhopH2 and Clag9 were detected; however, Clag2 and -3.1 were not, indicating that Clag9 does not form a complex with these RhopH1/Clag members. *Anti*-SERA5 serum did not detect any signal in the *anti*-RhopH2 immunoprecipitate, thereby excluding any potential carryover due to insufficient or inadequate washing steps.

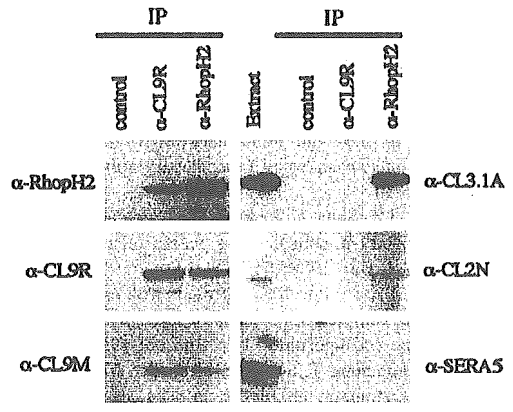

Fig. 7. Clag2, -3.1, and -9 are components of the RhopH complex, however, Clag2 and -3.1 do not form a complex with Clag9. Parasite extracts ('Extract') were immunoprecipitated ('IP') with rabbit *anti*-RhopH2 (α-RhopH2), *anti*-Clag9 (α-CL9R), or control normal sera and stained with rabbit *anti*-RhopH2, rabbit *anti*-Clag9 (α-CL9R), mouse *anti*-Clag9 (α-CL9M), rabbit *anti*-Clag3.1 (α-CL3.1A), rat *anti*-Clag2 (α-CL2N), or mouse *anti*-SERA5 sera.

4. Discussion

In this paper, we determined the cDNA sequences and transcription profiles of all five *rhoph1/clag* members throughout the asexual blood-stages of the *P. falciparum* life-cycle. Using a panel of specific antisera, the protein expression of Clag2 and -3.1 was demonstrated to be at the apical end of merozoites in segmented schizonts. Furthermore, these members were confirmed to be additional components of the RhopH complex, similar to Clag9 that we have previously shown to be apically expressed by IFA and localized to the rhoptry bodies by immunoelectron microscopy [20]. Clag2 and -3.1 appear not to be involved in RhopH complexes containing Clag9, suggesting that differing populations of RhopH complex exist, and each may contain only a single RhopH1/Clag member.

Initial releases of the *P. falciparum* genome sequence, and preliminary annotations contained numerous unassigned contigs, many of which were derived from "chromosome Blob"—a collective term representing chromosomes 6, 7, and 8, so-named due to the difficulty in separating these similarly-sized chromosomes. However, by linkage analysis we successfully located the gene locus for *clagb1* on the subtelomeric region of chromosome 8 and have consequently re-designated the gene '*clag8*' in accordance with its location. Once genomic DNA has been prepared from approximately 20 progeny of a *P. falciparum* genetic cross, linkage analysis is the most rapid and effective method of identifying a gene locus. The method employed in this report would assist the gap-closure process for further unassigned contigs.

Etzion et al. (1991) proposed that the PfRhopH complex would contain one each of RhopH1, RhopH2 and RhopH3, based on the estimated total molecular mass of the PfRhopH complex (approximately 480 kDa), which approximates to the sum of the individual molecular masses of RhopH1 (155 kDa), RhopH2 (140 kDa), and RhopH3 (110 kDa) [36]. This is consistent with our data showing that a RhopH complex containing Clag9 does not contain Clag2 or Clag3.1. Collectively, these data indicate that each RhopH complex contains only a single RhopH1/Clag member.

Phylogenetic analysis suggests that *rhoph1/clag* family members consist of two types, which were likely to have been created by a gene duplication event before speciation in the *Plasmodium* genus. Similar gene duplication events can be seen in other *Plasmodium* molecules, such as genes encoding ookinete surface proteins Pxs25 and Pxs28 or gametocyte surface proteins Pxs48 and Px47, which are tandemly located on the same chromosome, whereas Type-A and -AP of *rhoph1/clag* genes are located on separate chromosomes. This ancient branching between Type-A and -AP subgroups is potentially responsible for the different timing of the start of transcription between *clag9* and other members presented in Fig. 3, though the biological relevance still remains unclear.

Interestingly Type-A of the *rhoph1/clag* family was further duplicated in *P. falciparum* and *P. vivax*, but Type-AP

was not. One might speculate that the location on the chromosome generates this difference. For example, genes located on the subtelomeric region such as erythrocyte-binding-like (*ebl*), reticulocyte-binding-like (*rbl*), and *var* families are frequently multiplied. However, since *clag9* is also located in the subtelomeric region of the chromosome (similar to the other four *rhoph1/clag* members) this is unlikely to be the case. Another possibility is a selective advantage of the gene duplication of Type-A *rhoph1/clag* members due to an unknown function important to parasite survival. Other *Plasmodium* multigene family products involved in erythrocyte invasion increase the redundancy in recognition of the erythrocyte surface receptors, which is advantageous to parasite survival. For example, the *ebl* family was multiplied independently in *P. falciparum* and *P. knowlesi* and each member protein has different specificity to host erythrocyte receptors [37–41]. Because the RhopH complex has the ability to bind erythrocytes [11,42], and each RhopH complex is likely to contain only a single RhopH1/Clag member, it is plausible that RhopH1/Clag members function as a ligand domain of the RhopH complex and Type-A members are more important than Type-AP members. The reduced importance of the *clag9* gene is further supported by the observation that a panel of culture-adapted *P. falciparum* clones do not retain the *clag9* gene ([43], unpublished data). Whether the deletion of the *clag9* gene locus is an in vitro artifact or a commonly occurring natural event in the wild-type parasite population remains to be ascertained.

Malaria parasites utilize a number of transcriptional regulation mechanisms to escape host immunity. An example of this is the *P. yoelii rbl* family, *py235*. Transcripts of different *py235* members have been detected from individual merozoites in a single schizont [44]. We questioned whether this is also the case for the *rhoph1/clag* family members in *P. falciparum*. However, this appears to be unlikely since immunofluorescence microscopy with specific antisera indicates that all merozoites in a single schizont express at least three RhopH1/Clag members.

In summary, it is now evident that at least three RhopH1/Clag members are components of the RhopH complex, which suggests that the remaining two members (Clag3.2 and Clag8) are also RhopH complex components. Based on the molecular mass of the RhopH complex and the lack of Clag2 or Clag3.1 in the RhopH complex containing Clag9, we propose that each RhopH complex likely contains only a single RhopH1/Clag member, suggesting five different types of *P. falciparum* RhopH complex. It is therefore of interest to explore the binding specificity of each RhopH complex, as this would create further redundancy in erythrocyte invasion by *P. falciparum* merozoites.

Acknowledgements

We thank K. Okugawa and K. Oka in the Integrated Center for Science, Ehime University for their expertise, S. Takeji for sequencing and S. Ogun, NIMR, for her assistance with immunizations. We also thank J. Mullins for providing pJW4304 and T. Horii for the mouse *anti*-SERA5 serum. Preliminary sequence data for *P. vivax* was obtained from The Institute for Genomic Research website at http://www.tigr.org. Animal experiments in this study were carried out in compliance with the Guide for Animal Experimentation at Ehime University School of Medicine, and under certification of the UK Home Office Animals (Scientific Procedures) Act 1986. This work was supported in part by Grants-in-Aid for Scientific Research 14370084 and 15406015 (to M. T.) and Encouragement of Young Scientists 15790215 (to O.K.) from the Ministry of Education, Culture, Sports, Science and Technology, Japan. B.Y.S.Y.L. acknowledges the support of a Medical Research Council (UK) PhD Studentship.

References

[1] Freeman RR, Trejdosiewicz AJ, Cross GAM. Protective monoclonal antibodies recognizing stage-specific merozoite antigens of a rodent malaria parasite. Nature 1980;284:366–8.
[2] Holder AA, Freeman RR. Immunization against blood-stage rodent malaria using purified parasite antigens. Nature 1981;294:361–4.
[3] Campbell GH, Miller LH, Hudson D, Franco EL, Andrysiak PM. Monoclonal antibody characterization of *Plasmodium falciparum* antigens. Am J Trop Med Hyg 1984;33:1051–4.
[4] Holder AA, Freeman RR, Uni S, Aikawa M. Isolation of a *Plasmodium falciparum* rhoptry protein. Mol Biochem Parasitol 1985;14:293–303.
[5] Lustigman S, Anders RF, Brown GV, Coppel RL. A component of an antigenic rhoptry complex of *Plasmodium falciparum* is modified after merozoite invasion. Mol Biochem Parasitol 1988;30:217–24.
[6] Hienne R, Ricard G, Fusaï T, et al. *Plasmodium yoelii*: identification of rhoptry proteins using monoclonal antibodies. Exp Parasitol 1998;90:230–5.
[7] Siddiqui WA, Tam LQ, Kramer KJ, et al. Merozoite surface coat precursor protein completely protects *Aotus* monkeys against *Plasmodium falciparum* malaria. Proc Natl Acad Sci USA 1987;84:3014–8.
[8] Cooper JA, Ingram LT, Bushell GR, et al. The 140/130/105 kDa protein complex in the rhoptries of *Plasmodium falciparum* consists of discrete polypeptides. Mol Biochem Parasitol 1988;29:251–60.
[9] Doury JC, Bonnefoy S, Roger N, Dubremetz JF, Mercereau-Puijalon O. Analysis of the high molecular weight rhoptry complex of *Plasmodium falciparum* using monoclonal antibodies. Parasitology 1994;108:269–80.
[10] Sam-Yellowe TY, Shio H, Perkins ME. Secretion of *Plasmodium falciparum* rhoptry protein into the plasma membrane of host erythrocytes. J Cell Biol 1988;106:1507–13.
[11] Sam-Yellowe TY, Perkins ME. Interaction of the 140/130/110 kDa rhoptry protein complex of *Plasmodium falciparum* with the erythrocyte membrane and liposomes. Exp Parasitol 1991;73:161–71.
[12] Hiller NL, Akompong T, Morrow JS, Holder AA, Haldar K. Identification of a stomatin orthologue in vacuoles induced in human erythrocytes by malaria parasites. A role for microbial raft proteins in apicomplexan vacuole biogenesis. J Biol Chem 2003;278:48413–21.
[13] Ling IT, Kaneko O, Narum DL, et al. Characterisation of the *rhoph2* gene of *Plasmodium falciparum* and *Plasmodium yoelii*. Mol Biochem Parasitol 2003;127:47–57.
[14] Cowman AF, Baldi DL, Healer J, et al. Functional analysis of proteins involved in *Plasmodium falciparum* merozoite invasion of red blood cells. FEBS Lett 2000;476:84–8.

[15] Brown HJ, Coppel RL. Primary structure of a *Plasmodium falciparum* rhoptry antigen. Mol Biochem Parasitol 1991;49:99–110.
[16] Shirano M, Tsuboi T, Kaneko O, Tachibana M, Adams JH, Torii M. Conserved regions of the *Plasmodium yoelii* rhoptry protein RhopH3 revealed by comparison with the *P. falciparum* homologue. Mol Biochem Parasitol 2001;112:297–9.
[17] Kaneko O, Tsuboi T, Ling IT, et al. The high molecular mass rhoptry protein, RhopH1, is encoded by members of the *clag* multigene family in *Plasmodium falciparum* and *Plasmodium yoelii*. Mol Biochem Parasitol 2001;118:237–45.
[18] Holt DC, Gardiner DL, Thomas EA, et al. The cytoadherence linked asexual gene family of *Plasmodium falciparum*: are there roles other than cytoadherence? Int J Parasitol 1999;29:939–44.
[19] Trenholme KR, Gardiner DL, Holt D, et al. *clag9*: a cytoadherence gene in *P. falciparum* essential for binding parasitized erythrocytes to CD36. Proc Natl Acad Sci USA 2000;97:4029–33.
[20] Ling IT, Florens L, Dluzewski AR, et al. The *Plasmodium falciparum clag9* gene encodes a rhoptry protein that is transferred to the host erythrocyte upon invasion. Mol Microbiol 2004;52:107–18.
[21] Su X, Kirkman LA, Fujioka H, Wellems TE. Complex polymorphisms in an approximately 330 kDa protein are linked to chloroquine-resistant *P. falciparum* in Southeast Asia and Africa. Cell 1997;28(91):593–603.
[22] Trager W, Jensen JB. Human malaria parasites in continuous culture. Science 1976;193:673–5.
[23] Staalsoe T, Giha HA, Dodoo D, Theander TG, Hviid L. Detection of antibodies to variant antigens on *Plasmodium falciparum*-infected erythrocytes by flow cytometry. Cytometry 1999;35:329–36.
[24] Taylor HM, Grainger M, Holder AA. Variation in the expression of a *Plasmodium falciparum* protein family implicated in erythrocyte invasion. Infect Immun 2002;70:5779–89.
[25] Su X, Ferdig MT, Huang Y, et al. A genetic map and recombination parameters of the human malaria parasite *Plasmodium falciparum*. Science 1999;286:1351–3.
[26] Kimura M, Kaneko O, Liu Q, et al. Identification of the four species of human malaria parasites by nested PCR that targets various sequences in the small subunit rRNA gene. Parasitol Int 1997;46:91–5.
[27] Lu S, Arthos J, Montefiori DC, et al. Simian immunodeficiency virus DNA vaccine trial in macaques. J Virol 1996;70:3978–91.
[28] Kaneko O, Mu J, Tsuboi T, Su X, Torii M. Gene structure and expression of a *Plasmodium falciparum* 220-kDa protein homologous to the *Plasmodium vivax* reticulocyte binding proteins. Mol Biochem Parasitol 2002;121:275–8.
[29] Pang XL, Mitamura T, Horii T. Antibodies reactive with the N-terminal domain of *Plasmodium falciparum* serine repeat antigen inhibit cell proliferation by agglutinating merozoites and schizonts. Infect Immun 1999;67:1821–7.
[30] Thompson JD, Higgins DG, Gibson TJ. CLUSTAL W: improving the sensitivity of progressive multiple sequence alignment through sequence weighting, position-specific gap penalties and weight matrix choice. Nucleic Acids Res 1994;22:4673–80.
[31] Saitou N, Nei M. The neighbor-joining method: a new method for reconstructing phylogenetic trees. Mol Biol Evol 1987;4:406–25.
[32] Kimura M. A simple method for estimating evolutionary rate of base substitutions through comparative studies of nucleotide sequences. J Mol Evol 1980;16:111–20.
[33] Page RD. TreeView: an application to display phylogenetic trees on personal computers. Comput Appl Biosci 1996;12:357–8.
[34] Le Roch KG, Zhou Y, Blair PL, et al. Discovery of gene function by expression profiling of the malaria parasite life cycle. Science 2003;301:1503–8.
[35] PlasmoDB: An integrative database of the *Plasmodium falciparum* genome. Tools for accessing and analyzing finished and unfinished sequence data. Nucleic Acids Res 2001; 29:66–9.
[36] Etzion Z, Murray MC, Perkins ME. Isolation and characterization of rhoptries of *Plasmodium falciparum*. Mol Biochem Parasitol 1991;47:51–61.
[37] Adams JH, Hudson DE, Torii M, et al. The Duffy receptor family of *Plasmodium knowlesi* is located within the micronemes of invasive malaria merozoites. Cell 1990;63:141–53.
[38] Adams JH, Kaneko O, Blair PL, Peterson DS. An expanding *ebl* family of *Plasmodium falciparum*. Trends Parasitol 2001;17:297–9.
[39] Mayer DC, Kaneko O, Hudson-Taylor DE, Reid ME, Miller LH. Characterization of a *Plasmodium falciparum* erythrocyte-binding protein paralogous to EBA-175. Proc Natl Acad Sci USA 2001;98:5222–7.
[40] Gilberger TW, Thompson JK, Triglia T, et al. A novel erythrocyte binding antigen-175 paralogue from *Plasmodium falciparum* defines a new trypsin-resistant receptor on human erythrocytes. J Biol Chem 2003;278:14480–6.
[41] Mayer DC, Mu JB, Kaneko O, Duan J, Su XZ, Miller LH. Polymorphism in the *Plasmodium falciparum* erythrocyte-binding ligand JESEBL/EBA-181 alters its receptor specificity. Proc Natl Acad Sci USA 2004;101:2518–23.
[42] Rungruang T, Kaneko O, Murakami Y, et al. Erythrocyte surface glycosylphosphatidyl inositol anchored receptor for the malaria parasite. Mol Biochem Parasitol 2005;140:13–21.
[43] Day KP, Karamalis F, Thompson J, et al. Genes necessary for expression of a virulence determinant and for transmission of *Plasmodium falciparum* are located on a 0.3-megabase region of chromosome 9. Proc Natl Acad Sci USA 1993;90:8292–6.
[44] Preiser PR, Jarra W, Capiod T, Snounou G. A rhoptry-protein-associated mechanism of clonal phenotypic variation in rodent malaria. Nature 1999;398:618–22.

Available online at www.sciencedirect.com
SCIENCE DIRECT®
Experimental Parasitology 109 (2005) 7–15
Experimental Parasitology
www.elsevier.com/locate/yexpr

Investigating serum factors promoting erythrocytic growth of *Plasmodium falciparum*

Hiroko Asahi[a,*], Tamotsu Kanazawa[b], Nakami Hirayama[c], Yousei Kajihara[d]

[a] *Department of Parasitology, National Institute of Infectious Diseases, 23-1 Toyama 1-chome, Shinjuku-ku, Tokyo 162-8640, Japan*
[b] *Department of Parasitology and Tropical Medicine, University of Occupational and Environmental Health, Iseigaoka 1-1, Yahata-nishiku, Kitakyusyu 807-8555, Japan*
[c] *Department of Immunology, National Institute of Infectious Diseases, 23-1 Toyama 1-chome, Shinjuku-ku, Tokyo 162-8640, Japan*
[d] *Life Tech Division, Nihon Pharmaceutical Co. Ltd., Sumiyoshi-cho 26, Izumisano, Osaka 598-0061, Japan*

Received 11 May 2004; received in revised form 16 October 2004; accepted 19 October 2004
Available online 10 December 2004

Abstract

The elucidation of factors inducing the growth of *Plasmodium falciparum* can provide critical information about the developmental mechanisms of this parasite and open the way to search for novel targets for malaria chemotherapy. The ability of components of a growth-promoting factor derived from bovine serum and various related substances to sustain growth of *P. falciparum* was characterized. A simple total lipid fraction (GFS-C) containing non-esterified fatty acids (NEFAs) as essential factors was noted to promote the parasite's growth. Various proteins from a variety of animals were tested, indicating the importance not only of GFS-C, but also of specific proteins, such as bovine and human albumin, in the parasite growth. Several combinations of the NEFAs tested sustained low parasite growth. Among various phospholipids and lysophospholipids tested, lysophosphatidylcholine containing C-18 unsaturated fatty acids was found to sustain the complete development of the parasite in the presence of bovine albumin. Several other lysophospholipids can partially support growth of *P. falciparum*.
© 2004 Elsevier Inc. All rights reserved.

Index Descriptors and Abbreviations: ALB, albumin; ANOVA, multifactorial analysis of variance; BSAF, NEFA-free ALB from bovine; C16:0, hexadecanoic acid; C16:1, *cis*-9-hexadecenoic acid; C18:0, octadecanoic acid; C18:1, *cis*-9-octadecenoic acid; C18:2, *cis,cis*-9,12-octadecadienoic acid; C18:3, *cis,cis,cis*-6,9,12-octadecatrienoic acid; C20:4, *cis*-5,8,11,14-eicosatetraenoic acid; C20:5, *cis*-5,8,11,14,17-eicosapentaenoic acid; C22:6, *cis*-4,7,10,13,16,19-docosahexaenoic acid; CDKs, cyclin-dependent protein kinases; CDPKs, calcium-dependent protein kinases; CHOL, cholesterol; CRPMI, basal medium; DGs, diglycerides; FBS, fetal bovine serum; GFS, a growth-promoting fraction derived from adult bovine serum; GFS-C, a total simple lipid fraction obtained from GFS; GFSRPMI, CRPMI containing 10% GFS; GFS-WM, a total complex lipid fraction obtained from GFS; Hepes, 4-(2-hydroxyethyl)-piperazine ethanesulfonic acid; HS, human serum; HSRPMI, CRPMI containing 10% HS; LPA, lysophosphatidic acid; 18:1 LPA, *cis*-9-oleoyl LPA; LPC, lysophosphatidylcholine; 12:0 LPC, lauroyl LPC; 14:0 LPC, myristoyl LPC; 16:0 LPC, palmitoyl LPC; 18:0 LPC, stearoyl LPC; 18:1 LPC, *cis*-9-oleoyl LPC; 18:2 LPC, *cis*-9-linoleoyl LPC; 18:U LPC, LPC containing primarily C-18 unsaturated fatty acids; LPC-brain, LPC from bovine brain; LPCRPMI, CRPMI containing 3 mg/ml BSAF and 40 μg/ml 18:U LPC; LPE, lysophosphatidyl ethanolamine; LPI, lysophosphatidyl inositol; LPS, lysophosphatidyl serine; Lyso PAF, γ-*O*-alkyl LPC; MAPK, mitogen-activated protein kinase; MEK, MAPK/extracellular signal-regulated kinase kinase; MGs, monoglycerides; NEFA, non-esterified fatty acid; OD_{650}, absorbance at 650 nm; 8:0 PA, dioctanoyl phosphatidic acid; 18:1 PA, *cis*-9-dioleoyl phosphatidic acid; PAF, β-acetyl-γ-*O*-alkyl PC; PC, phosphatidylcholine; PE, phosphatidyl ethanolamine; PI, phosphatidyl inositol; PI-bovine, PI from bovine liver; PI-soybean, PI from soybean; PKC, protein kinase C; PLs, phospholipids; pLDH, parasite lactate dehydrogenase; PS, phosphatidyl serine; PTK, protein tyrosine kinase; RBCs, red blood cells; SD, standard deviation; SM, sphingomyelin; S-1-P, sphingosine 1-phosphate; SPC, sphingosylphosphorylcholine; sphingosine, D- sphingosine
Keywords: Protozoan *Plasmodium falciparum*; Growth-promoting factor; Simple total lipids; Lysophospholipids

* Corresponding author. Fax: +81 3 5285 1150.
E-mail address: asahih@nih.go.jp (H. Asahi).

0014-4894/$ - see front matter © 2004 Elsevier Inc. All rights reserved.
doi:10.1016/j.exppara.2004.10.002

1. Introduction

Malaria remains a devastating disease, particularly in the Tropics. The estimated incidence of malaria in the world is of the order of 300–500 million clinical cases annually. The annual estimates of malaria mortality, particularly those caused by the protozoan *Plasmodium falciparum*, vary from 1.5 to 2.7 million worldwide (WHO, 1997). The efficacy of conventional antimalarial drugs and insecticides in controlling malaria outbreaks is declining, with increasing resistance of parasites and their vectors. This highlights the need to develop new chemotherapeutic approaches based on a better understanding of parasite biology and its interaction with the host.

The continuous in vitro cultivation of *P. falciparum* erythrocytic stages represented a significant advance in malaria research (Trager and Jenson, 1978). Despite considerable advances in understanding the molecular and genetic characteristics of this protozoan (PlasmoDB, http://www.plasmodb.org), the mechanisms responsible for *P. falciparum* growth remain largely unknown. It has been suggested that *P. falciparum* requires some factors present in human serum (HS), although the role of HS in the growth of this parasite is still unknown. When only dialyzable factors of HS (low-molecular-mass compounds) are present in the commonly employed basic medium, RPMI1640, the parasite fails to develop from rings to schizonts, but good growth is observed by adding non-dialyzable HS factors (Jensen, 1979).

We previously reported a growth-promoting fraction derived from adult bovine serum (GFS) that yields good intraerythrocytic *P. falciparum* growth (Asahi and Kanazawa, 1994). In addition, a low-molecular-weight factor that is of importance in serum-free media was clearly shown to be a purine precursor, such as hypoxanthine, adenine or adenosine (Asahi et al., 1996; Divo and Jensen, 1982). It is essential but not sufficient for the optimum parasite growth (Asahi et al., 1996). GFS is a 55–70% ammonium sulfate fraction of adult bovine serum, and contains lipid-rich albumin (ALB) as a major component (Kudo et al., 1987). Similarly, Cranmer et al. (1997) reported that commercially available lipid-enriched bovine ALB (Albumax II; Gibco-BRL Life Technology, USA) can replace HS for the continuous in vitro cultivation of *P. falciparum*. Consequently, data are still too crude to allow direct identification of the functional factors required for the growth of *P. falciparum*.

The replacement of HS in a culture medium with chemically or functionally defined substances would not only be advantageous for the culture of the parasite, but it also provides critical clues to a thorough understanding of the parasite's proliferation at the erythrocyte stage, and may lead to the identification of novel targets for malaria chemotherapy. Therefore, this study was undertaken to characterize the ability of the components of GFS and various related substances to sustain parasite growth.

2. Materials and methods

2.1. Parasite, culture, and synchronization

Cultures of the FCR/FMG (ATCC Catalogue No. 30932, Gambia) strain of *P. falciparum* were used in the experiments. Parasites were routinely maintained by in vitro culture techniques using culture medium free of whole serum, consisting of basal medium (CRPMI) supplemented with 10% GFS (Wako Pure Chemical Industries, Japan, under the trade name Daigo's GF21), as previously reported (Asahi et al., 1996). This complete medium is termed GFSRPMI. CRPMI consists of RPMI1640 containing 2 mM glutamine, 25 mM 4-(2-hydroxyethyl)-piperazine ethanesulfonic acid (Hepes), and 24 mM $NaHCO_3$ (Gibco-BRL Life Technology, USA), 25 μg/ml gentamycin (Sigma Chemical, USA), and 150 μM hypoxanthine (Sigma). Briefly, red blood cells (RBCs), which were preserved in Alsever's solution (Asahi et al., 1996) for 3–30 days, were washed, dispensed in a 24-well culture plate at a hematocrit of 2% (1 ml of suspension/well), and cultured under a humidified atmosphere of 5% CO_2, 5% O_2, and 90% N_2 at 37 °C. For subculture, 4 days after inoculation, infected and uninfected RBCs were washed with CRPMI. Parasitemia was adjusted to 0.1% (for subcultures) or 0.4% (for growth tests) by adding uninfected RBCs, and hematocrit adjusted to 2% by adding the appropriate volume of culture medium, either GFSRPMI or the medium to be tested.

Cultures were occasionally synchronized by two successive exposures at 34–38-h intervals to 5% (w/v) D-sorbitol (Asahi and Kanazawa, 1994).

2.2. Growth-promoting activity experiments

The growth experiments were performed by replacing GFSRPMI with CRPMI supplemented with the substances to be tested. The following were tested for their growth-promoting activity: 10% (v/v) heat-inactivated HS (O-type) (HSRPMI); 2.5–10% heat-inactivated fetal bovine serum (FBS); 3 mg/ml non-esterified fatty acid (NEFA)-free ALB from bovine (BSAF), human, porcine, ovine, guinea pig or equine serum; and 3 mg/ml ovalbumin, lactoglobulin, lysozyme, and casein (Merck, Germany). CRPMI containing BSAF at a final concentration of 3 mg/ml, except when otherwise stated, was further supplemented with graded concentrations of: hexadecanoic acid (palmitic acid, C16:0); *cis*-9-hexadecenoic acid (palmitoleic acid, C16:1); octadecanoic acid (stearic acid, C18:0); *cis*-9-octadecenoic acid (oleic acid, C18:1); *cis,cis*-9,12-octadecadienoic acid (linoleic acid, C18:2); *cis,cis,cis*-

6,9,12-octadecatrienoic acid (γ-linolenic acid, C18:3); *cis*-5,8,11,14-eicosatetraenoic acid (arachidonic acid, C20:4); *cis*- 5,8,11,14,17-eicosapentaenoic acid (C20:5); *cis*-4,7,10,13,16,19-docosahexaenoic acid (C22:6); palmitoyl lysophosphatidyl serine (LPS), sodium salt; soybean lysophosphatidyl inositol (LPI) containing primarily C18:0 and C16:0; egg yolk lysophosphatidyl ethanolamine (LPE) containing primarily C18:0 and C16:0; lysophosphatidylcholine (LPC), γ-*O*-alkyl, from bovine heart (Lyso-oPAF); lysophosphatidic acid (LPA), *cis*-9-oleoyl (18:1 LPA), sodium salt (Biomol Research Laboratory, USA); soybean LPC containing primarily C-18 unsaturated fatty acids (18:U LPC); lauroyl LPC (12:0 LPC); myristoyl LPC (14:0 LPC); palmitoyl LPC (16:0 LPC); stearoyl LPC (18:0 LPC); *cis*-9-oleoyl LPC (18:1 LPC); *cis*-9-linoleoyl LPC (18:2 LPC, Doosan Serdary Research Lab, USA); LPC from bovine brain (LPC-brain); sphingosylphosphorylcholine (lysosphingomyelin) (SPC); phosphatidylcholine (PC) from egg yolk; phosphatidyl serine (PS) from bovine brain; phosphatidyl ethanolamine (PE) containing primarily C18:1 and C16:0; phosphatidyl inositol (PI) containing primarily C18:1 and C16:0, from soybean (PI-soybean); bovine liver PI (PI-bovine), ammonium salt; β-acetyl-γ-*O*-alkyl PC (PAF); sphingosine 1-phosphate (S-1-P); D-sphingosine (sphingosine) from bovine brain sphingomyelin (SM); egg yolk SM containing primarily C16:0; dioctanoyl phosphatidic acid (8:0 PA), sodium salt; or *cis*-9-dioleoyl phosphatidic acid (18:1 PA), sodium salt. CRPMI supplemented with BSAF (3 mg/ml) and 18:U LPC (40 μg/ml) is termed LPCRPMI. Unless otherwise stated, all compounds were obtained from Sigma. Parasites were cultured for 4 days after inoculation (two cycles of complete growth), except when otherwise stated.

For the reconstitution of lipids, dried lipid precipitates were prepared by evaporating the organic solvent from lipid stock solutions in acetone or a mixture of chloroform and methanol by centrifugation under vacuum. CRPMI containing proteins, except when otherwise stated, was added to the dried lipid precipitates, and the mixtures were sonicated for 5 min and sterilized using a 0.45-μm filter.

2.3. Assessment of parasite growth

Samples were obtained at the times indicated. Smears were prepared and stained with Giemsa. More than 10,000 RBCs were examined to determine parasitemia. The growth rate was first estimated by dividing the parasitemia of the test sample 4 days after inoculation by the initial parasitemia, except when otherwise stated. Further measurement of growth rates was performed using the parasite lactate dehydrogenase (pLDH) assay (Makler and Hinrichs, 1993), in cultures containing growth promoters such as HS, GFS, GFS-C, 18:U LPC, and 18:1 LPA. The Malstat reagent (Flow, USA) was used as an indicator of parasite viability, and the pLDH assay was performed according to the manufacturer's instruction. Briefly, at the incubation times indicated, the RBCs in cultures were hemolyzed by three freeze–thaw cycles, and 10 μl of infected erythrocyte was transferred to each well of a 96-well microtiter plate. Then 100 μl of the Malstat reagent, 10 μl of 1 mg/ml nitroblue tetrazolium (Wako) and 10 μl of 1 mg/ml diaphorase (Wako) were added to each well. The plate was allowed to stand for 40 min at 37 °C, and the reaction was stopped by the addition of 50 μl of 5% (v/v) acetic acid. The absorbance at 650 nm (OD_{650}) was read on a plate reader. The initial OD_{650} value measured at the addition of assay reagents was subtracted from the endpoint reading. For each experiment, parasitized RBCs were divided into identical aliquots, and different treatments were performed simultaneously. To make the results comparable across experiments, external untreated control wells, namely cultures in GFSRPMI and HSRPMI, were set up each time. In all the experiments, culture wells were run in triplicate.

2.4. Separation and analysis of lipids

Known amounts of GFS were extracted by the method of Bligh and Dyer (Asahi et al., 1986). The fractions obtained, namely, the chloroform (total simple lipid fraction, GFS-C) and water–methanol (total complex lipid fraction, GFS-WM) fractions, were further evaporated. They were suspended in the original volume of the culture medium for assay of growth-promoting activity on the parasite.

GFS-C was further separated by thin-layer chromatography using petroleum ether–diethylether–acetic acid (80:30:1, by volume) as a developing solvent system, as described previously (Asahi et al., 1986).

Gas–liquid chromatography of NEFAs was performed as described previously (Asahi et al., 1986).

2.5. Statistical analysis

Statistical significance for differences was evaluated using multifactorial analysis of variance (ANOVA). All calculations were performed using StatView 5.0J software (SAS Institute, USA). The P value for significance was 0.05, and all pairwise comparisons were made post hoc with Bonferroni/Dunn's test. For graphical representation of the data, y-axis error bars indicate the standard deviation (SD) of the data for each point on the figure.

3. Results

3.1. Essential GFS factors for P. falciparum growth

After extraction of lipids from GFS, GFS-C, and GFS-WM and a mixture of the two fractions were tested

for their ability to sustain parasite growth. GFS-C and the GFS-C + GFS-WM mixture exhibited growth-promoting activity only in the presence of BSAF (Fig. 1A). The parasites retained their normal morphology and gametocytes were rarely recognized. Neither BSAF nor GFS-C alone sustained parasite growth (Fig. 1A). GFS-C was further separated by thin-layer chromatography. The fractions including phospholipids (PLs), diglycerides (DGs), cholesterol (CHOL), monoglycerides (MGs), NEFAs, and CHOL-ester, and their mixtures were assayed for their growth-promoting ability in the presence of BSAF. The parasite growth was promoted only in the presence of NEFAs or mixtures containing NEFAs, although the extent of growth was much less than that for GFS-C + BSAF, GFS-C + GFS-WM + BSAF, GFSRPMI, and HSRPMI (Figs. 1A and B). These results imply that GFS-C containing NEFAs as essential factors was the functional factor inducing parasite growth. However, other factors contributing to the growth-promoting activity of GFS should not be ruled out.

To determine whether proteins other than BSAF can sustain parasite growth, *P. falciparum* was cultured with GFS-C and various proteins. The parasite growth in the culture medium enriched with human ALB was similar to that of medium supplemented with BSAF. Guinea pig, ovine, equine, and porcine ALB also supported parasite growth, but to a lesser extent (Fig. 2A). The addition of ovalbumin, lactoglobulin, lysozyme, and casein to the culture medium enriched with GFS-C did not promote parasite growth. To determine the optimum protein concentration for growth of *P. falciparum*, BSAF or human ALB at different concentrations was added to the culture medium enriched with GFS-C. Relatively high concentrations of protein (0.75–3 mg/ml BSAF and 3 mg/ml human ALB) were necessary for the optimum parasite growth (Fig. 2B). These results indicate the importance not only of lipids (GFS-C), but also of proteins in promoting and sustaining parasite growth.

The components of the NEFA fraction of GFS-C were further analyzed by gas–liquid chromatography to identify the acids involved. The NEFA fraction was shown to contain mainly C18:1 (43%), C16:0 (21%), C18:0 (14%), C18:2, C16:1, C20:4, C20:5, and C22:6, which are commonly found in human and bovine sera (Manku et al., 1983). Each of the commercially available NEFAs enriched with BSAF was tested, either individually or in mixtures, for their ability to promote parasite growth. Individual NEFAs combined with BSAF did not promote parasite growth. In contrast, mixtures of NEFAs, such as C16:0 + C18:1, C16:0 + C18:1 + C22:6, and C16:0 + C18:0 + C18:1 + C18:2, promoted parasite growth, although the growth rate was much lower than that for GFS-C + BSAF, GFSRPMI, and HSRPMI (Fig. 3).

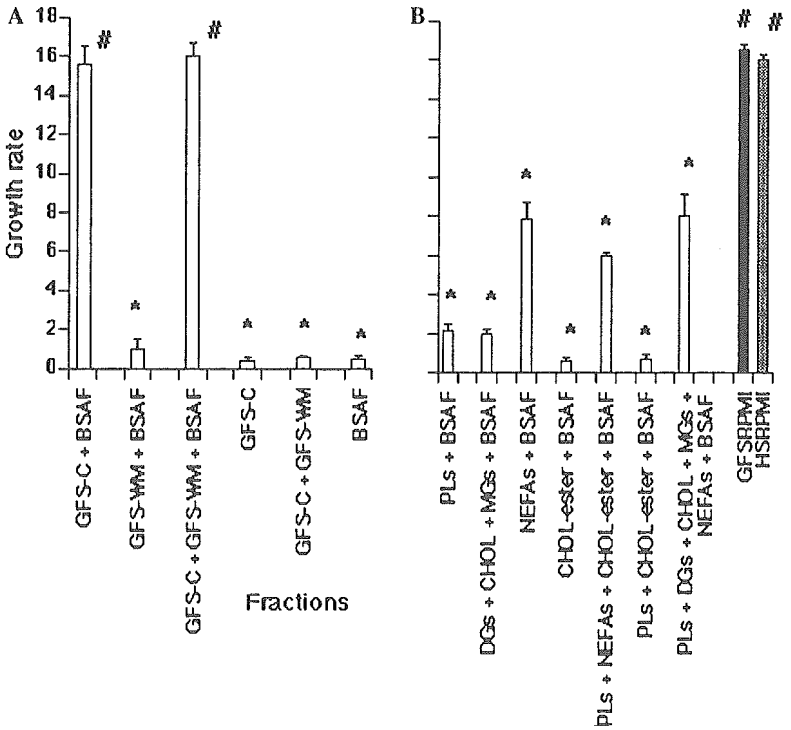

Fig. 1. Ability of: (A) fractions derived from GFS and (B) simple-lipid fractions derived from GFS-C to sustain growth of *P. falciparum*. The culture media contained 3 mg/ml BSAF, except for GFS-C, GFS-C + GFS-WM, GFSRPMI, and HSRPMI, which are shown for comparison. Growth rate was determined as described in Materials and methods. *Significant difference ($P < 0.001$) versus GFS-C + BSAF; versus GFS-C + GFS-WM + BSAF; versus GFSRPMI; versus HSRPMI. #No significant difference. These experiments were repeated twice, with similar results.